From the Department of Neuroscience
Karolinska Institutet, Stockholm, Sweden

MITOCHONDRIAL DNA MUTATIONS. BRAIN DEVELOPMENTAL AND AGEING CONSEQUENCES, AND POSSIBLE TREATMENTS

Jaime M. Ross

Karolinska Institutet

Stockholm 2012

Back Cover: *Looking Through Time,* vine charcoal by Jaime M. Ross (1993).

Front Cover: *Ålderstrappan,* painting on fabric by Winter Carl Hansson (1777-1805). Photo: Sören Hallgren / Leksands Local Historical Archives. Scripture (Job, 14.1-2): *Menniskan af qwinno föd lefwer en liten tid och är full med orolighet wäxser up som ett blåmster och faller af flyr bårtt som en skugge och blifwer icke.* (*Man that is born of a woman is of few days, and full of trouble. He cometh forth like a flower, and is cut down: he fleeth also as a shadow, and continueth not.*).

Published by Karolinska University Press
Box 200, SE-171 77 Stockholm, Sweden
Printed by Larserics Digital Print AB

ISBN 978-91-7457-843-0

Senectus ipsa morbus est
(Old Age in itself is a disease)
– P. Terentius Afer, *Phormio*

ABSTRACT

Ageing is a complex process that involves cellular senescence, a gradual loss of tissue homeostasis, and decline in organ function. Abundant evidence implicates mitochondria in ageing suggesting: (i) accumulation of mitochondrial DNA (mtDNA) damage, (ii) progressive respiratory chain dysfunction, and (iii) increased reactive oxygen species production. The "Mitochondrial Theory of Aging", first proposed by Denham Harman in 1972, suggests that damage to mtDNA slowly accumulates with time and causes ageing phenotypes by interfering with bioenergetic homeostasis and/or by loss of cells because of apoptosis and/or cellular senescence. This theory is supported by a wealth of correlative data, but has remained controversial in the absence of experimental proof.

In this thesis, the first mouse model to experimentally address the "Mitochondrial Theory of Aging", the mtDNA mutator mouse, was used to study how elevated somatic mtDNA mutations might translate to age-related functional changes in the central nervous system. The mtDNA mutator mouse is a homozygous knock-in transgenic mouse model that expresses a proof-reading deficient version of the nucleus-encoded catalytic subunit of mtDNA polymerase-γ (PolgA). The model demonstrates a cause and effect relationship between slowly increasing somatic mtDNA mutation levels and several human-like phenotypes associated with ageing that are manifested much earlier in life.

There are few means to track symptomatic stages of brain ageing. Using both prematurely ageing mtDNA mutator mice and normally ageing mice, a molecular link was established between mitochondrial dysfunction and abnormal metabolism in the ageing process, resulting in marked increases in brain lactate levels, even before the appearance of overt ageing phenotypes. The lactate dehydrogenase (LDH) genes responsible for the interconversion of pyruvate-to-lactate, LDH-A and LDH-B, which generate the H and M subunits of the 5 different tetrameric LDH isoenzymes, were analyzed and the isoenzyme composition and activities were found to have changed in favor of pyruvate-to-lactate conversion (Paper I).

To correlate the striking increase in lactate with tissue histopathology, the activities of cytochrome *c* oxidase and succinate dehydrogenase were investigated. Failing respiratory chain function was found in key brain areas of mtDNA mutator mice, and, later in life, in normal mice (Papers I and II).

Endurance exercise has been recently found to counteract progeroid ageing in prematurely ageing mice similar to the mtDNA mutator mice. Thus, the effect of diet supplementation with natural ingredients, vitamins, and antioxidants was investigated as an alternative strategy. The lifespan of mtDNA mutator mice receiving the dietary supplement NT-020-BV was increased by approximately 12%. The onset of the progeroid ageing phenotypes, such as canities, alopecia, kyphosis, elongation of ears, reduced body size, and weight loss was also delayed, and the enlargement of organs and sarcopenia were ameliorated. Moreover, locomotion and gait, as well as motor programming were also improved in mtDNA mutator mice receiving an NT-020-BV-enriched diet (Paper IV).

In addition to developing a premature ageing syndrome, approximately 30% of mtDNA mutator mice also exhibit stochastic brain malformations, ranging from major local perturbations of brain organization to symmetrical hippocampal and cortical migration disturbances. However, such brain malformations were only seen if heterozygous ($PolgA^{mut/WT}$) females had been maintained as maternal lineages for several generations. Instead, when wild-type mtDNA was re-introduced by crossing heterozygotes with C57Bl/6 females, the resulting mtDNA mutator mice had no brain malformations. Furthermore, the reintroduction of wild-type mtDNA also improved fertility and viability of offspring, and also delayed the onset of ageing phenotypes. This suggests that the extent of mtDNA mutation load during embryogenesis may also predict the rate of ageing *per se* in mtDNA mutator mice (Paper III).

In summary, these results support a role for mtDNA mutation load and mitochondrial dysfunction in ageing as well as in neurodevelopment, and show that intervention with diet might combat such mitochondrial deficiencies in ageing.

LIST OF PUBLICATIONS

This thesis is based on the following articles and manuscripts that will be referred to in the text by their roman numerals:

I. **Ross JM**, Öberg J, Brené S, Coppotelli G, Terzioglu M, Pernold K, Goiny M, Sitnikov R, Kehr J, Trifunovic A, Larsson NG, Hoffer BJ, Olson L. (2010) High brain lactate is a hallmark of aging and caused by a shift in the lactate dehydrogenase A/B ration. *Proceedings of the National Academy of Sciences of the United States of America (PNAS).* 107(46): 20087-92.

II. **Ross JM**. (2011) Visualization of mitochondrial respiratory function using cytochrome *c* oxidase / succinate dehydrogenase (COX/SDH) double-labeling histochemistry. *Journal of Visualized Experiments (JoVE)*. (57), e3266.

III. **Ross JM**, Pernold K, Brené S, Larsson NG, Hoffer BJ, Olson L. Maternal inheritance of mtDNA mutations contribute to diverse brain malformations in mice homozygous for proof-deficient mitochondrial DNA polymerase. *Manuscript.*

IV. **Ross JM**, Bickford PC, Abrams MB, Codeluppi S, Hoffer BJ, Olson L. Natural substances counteract prematurely ageing phenotypes in mtDNA mutator mice. *Manuscript.*

OTHER PUBLICATIONS

- **Ross JM**, Coppotelli G, and Olson L. (2011) Reply to Quistorff and Grunnet: Dysfunctional mitochondria, brain lactate, and lactate dehydrogenase isoforms. *Proceedings of the National Academy of Sciences United States of America (PNAS)*. 108 (7): E22.

- Lin L, McCroskery S, **Ross JM**, Chak Y, Neuhuber B, Daniels MP. (2010) Induction of filopodia-like protrusions by transmembrane agrin: role of agrin glycosaminoglycan chains and Rho-family GTPases. *Experimental Cell Research.* 316(14): 2260-77.

TABLE OF CONTENTS

INTRODUCTION **1**

MITOCHONDRIA 1

Structure of mitochondria *2*

Cellular respiration *4*

Glycolysis 4

Tricarboxylic acid cycle 5

Oxidative phosphorylation 5

Mitochondrial DNA *7*

Replication of mitochondrial DNA 8

Reactive oxygen species *8*

Mitochondrial DNA mutations *9*

Mitochondrial disease *10*

AGEING 12

What is ageing per se? *12*

Theories on ageing *13*

Evolutionary views 13

Is ageing programmed? 14

Mitochondria and ageing 15

The mtDNA mutator mouse *17*

AIMS OF THE THESIS **19**

MATERIALS AND METHODS **20**

ANIMALS 20

The mtDNA mutator mouse *20*

Housing and diet *21*

IN VIVO TECHNIQUES 22

Magnetic resonance imaging *22*

Animal preparation 22

Inversion recovery imaging 22

^{1}H-Magnetic resonance spectroscopy 23

Locomotion *25*

Gait analysis *25*

Videography *27*

HISTOCHEMICAL-BASED TECHNIQUES 27

Tissue preparation for cryosectioning *27*

Histology *27*

Immunohistochemistry *27*

Enzyme histochemistry *28*

mRNA Expression *29*

Oligonucleotide probes 29

in situ Hybridization 29

Image analysis 30

Microscopy *30*

CHROMATOGRAPHIC-BASED TECHNIQUES 31
High-performance liquid chromatography *31*
Tissue preparation with blood 31
Tissue preparation with blood removed 31
Determination of lactate 31
ENZYMATIC CHARACTERIZATION TECHNIQUES 32
Tissue preparation *32*
Measurement of protein concentration *32*
Lactate dehydrogenase isoenzyme characterization *32*
Lactate dehydrogenase activity *33*
STATISTICS 34
RESULTS AND DISCUSSION **35**
LACTATE AS A BIOMARKER OF THE AGEING PROCESS (PAPER I) 35
VISUALIZATION OF MITOCHONDRIAL RESPIRATORY FUNCTION (PAPER I AND II) 37
ALTERATIONS IN LDH-A AND -B TRANSCRIPTIONAL ACTIVITIES (PAPER I) 40
POSSIBLE TREATMENTS TO COMBAT THE AGEING PROCESS (PAPER IV) 42
STOCHASTIC DISTURBANCES OF BRAIN DEVELOPMENT (PAPER III) 44
"Non-focal" brain disturbances *45*
"Focal" brain disturbances *46*
POSSIBLE SOURCES OF MITOCHONDRIAL DNA MUTATION LOAD (PAPER III) 47
THE IMPORTANCE OF STARTING LIFE WITH HEALTHY MITOCHONDRIA (PAPER III) 48
CONCLUSIONS **51**
CONCLUDING REMARKS **53**
ACKNOWLEDGEMENTS **56**
REFERENCES **59**

LIST OF ABBREVIATIONS

A	adenine
acetyl CoA	acetyl Coenzyme A
ATP	adenosine-5'-triphosphate
ADP	adenosine di-phosphate
ANOVA	analysis of variance
ANT	adenine nucleotide translocator
a.u.	arbitrary units
B	tesla
bp	base pair
BSA	bovine serum albumin
BW	bandwidth
C	cytosine
CA1	*Cornu Ammonis* subdivision 1 of hippocampus
CNS	central nervous system
COX	cytochrome *c* oxidase
CO I-III	cytochrome *c* oxidase subunit genes
CRLB	Cramér–Rao lower bounds
Cr + PCr	total creatine (creatine and phosphocreatine)
dATP	deoxyadenosine 5′-triphosphate
DAB	3,3'-diaminobenzidine tetrahydrochloride
EDTA	ethylenediaminetetraacetic acid
ETC	electron-transport chain
ETF	electron transfer flavoprotein
F	*Filial* (generation)
FAD	flavin adenine dinucleotide
$FADH_2$	flavin adenine dinucleotide (reduced form)
FOV	field of view
g	g-force
G	guanine
GC	guanine-cytosine
GFAP	glial fibrillary acidic protein
GTP	guanosine-5'-triphosphate

h	hour(s)
HPLC	high-performance liquid chromatography
i.p.	intraperitoneal (injection)
ISH	*in situ* hybridization
IU	international units
K_m	Michaelis constant
KOH	potassium hydroxide
L	lactate
LDH-A	lactate dehydrogenase A
LDH-B	lactate dehydrogenase B
LDH 1-5	lactate dehydrogenase isoenzyme 1-5
M	mean
MEFs	mouse embryonic fibroblasts
min	minute(s)
MRI	magnetic resonance imaging
mRNA	messenger RNA
mtDNA	mitochondrial DNA
NADH	nicotinamide adenine dinucleotide (reduced form)
NAD^+	nicotinamide adenine dinucleotide
NBT	nitroblue tetrazolium
ND	NADH dehydrogenase
nDNA	nuclear DNA
NT-020-BV	dietary supplement NT-020 plus BioVin®
Nurr1	nuclear receptor related 1 protein
OVS	outer volume suppression
OXPHOS	oxidative phosphorylation
P	p-value
P	pyruvate
P_i	inorganic phosphate
PBS	phosphate-buffered saline
PCR	polymerase chain reaction
PMS	phenazine methosulfate
POLγ	mitochondrial DNA polymerase-γ
PolgA	α-subunit of mitochondrial DNA polymerase-γ

PPB	potassium phosphate buffer
ppm	parts per million
PRESS	point-resolved spectroscopy
Q	coenzyme Q_{10}
RARE	rapid acquisition with relaxation enhancement
RC	respiratory chain
RF	radio frequency
rRNA	ribosomal RNA
RT	room temperature
ROS	reactive oxygen species
s	second(s)
SD	standard deviation
SDH	succinate dehydrogenase
SEM	standard error of the mean
SNR	signal-to-noise ratio
t	*t*-statistic
T	thymine
TdT	terminal deoxynucleotidyl transferase
TE	echo time
TR	repetition time
tRNA	transfer RNA
TCA	tricarboxylic acid
UCP	uncoupling protein
UV	ultra-violet
VAPOR	variable power RF pulses and optimized relaxation delays
VOI	volumes of interest
vol	volume
w	week(s)
wt	weight
WT	wild-type
^{1}H-MRS	proton-magnetic resonance spectroscopy
5'-dRP	5'-deoxyribose-5-phosphate
α	alpha significance level (statistics)
χ^2	chi-square

INTRODUCTION

The past decade has witnessed an explosion of knowledge regarding the molecular mechanisms underlying the ageing process and its modulation by genetic and lifestyle factors. This introduction aims to summarize the field of ageing research and its relationship to energy metabolism at such a pivotal point.

MITOCHONDRIA

The discovery of mitochondria was made 170 years ago, during the 1840s, only a few years after the discovery of the cell nucleus (reviewed in Ernster and Schatz 1981). Despite the long-standing recognition of these intracellular structures, the understanding of their function was revealed gradually, due to technical limitations. Richard Altmann, in 1890, established mitochondria as cell organelles and referred to them as “bioblasts”, concluding that they were separate organisms living inside the cells and providing vital functions (Ernster and Schatz 1981). The term “mitochondrion” was finally introduced fifty years later by Carl Benda in 1898; it originates from the Greek “mitos” meaning “thread” and “chondrion” meaning “granule”, referring to the appearance of these structures during spermatogenesis (Ernster and Schatz 1981). An additional twenty years passed until mitochondria were first associated with cell respiration in 1912 by B.F. Kingsbury, but these data were based almost exclusively on morphological observations without direct chemical evidence (Ernster and Schatz 1981). It wasn’t until the 1950s that mitochondria were finally recognized as being “the powerhouse of the cell”, as they are often referred to (Sickevitz 1957).

Almost all eukaryotic cells, including fungi, animals, and plants, contain mitochondria, an organelle present in the cytoplasm that produces energy in the form of adenosine triphosphate (ATP) from the oxidation of molecules, including proteins, lipids, and polysaccharides. ATP powers nearly all energy-dependent cellular processes. Additionally, mitochondria are involved in a range of other processes, including signaling, cellular differentiation, cell death, and the control of the cell cycle and cell

growth (McBride et al. 2006). It is hypothesized that aerobic eukaryotic cells evolved from symbiosis 1.5 – 2 billion years ago when aerobic eubacteria were engulfed by an ancestral anaerobic eukaryotic cell. This is known as the "Endosymbiotic Theory", first proposed by Konstantin Mereschkowski in 1905 (Mereschkowski 1905). These bacterial ancestors of mitochondria initiated a symbiotic relationship by exchanging large amounts of energy for shelter and nourishment from the cell (Margulis 1970). Approximately 10^9 molecules of ATP are found at any time per cell, and are turned over every 1-2 minutes (Alberts 2008).

Structure of mitochondria

Similar to its bacterial-ancestry, mitochondria are small in size and contain their own circular double-stranded genome (mtDNA), their own ribosomes, and their own transfer RNAs. Each cell contains hundreds of mitochondria and thousands of copies of mtDNA. Interestingly, the mtDNA found in human eukaryotic cells is a degenerate version of its corresponding bacterial genomes and consists of only 15,000-17,000 nucleotide pairs. Of the 37 genes, 13 encode proteins that are integral components of the respiratory chain, 22 encode transfer RNAs (tRNA), and 2 encode ribosomal RNA (rRNA) components (Alberts 2008). The missing genes, however, have not been lost, but have instead been transferred during symbiosis to the nuclear DNA (nDNA) of the host cell, which has acquired genes for the structure of the mitochondria (approximately 1000 proteins) (Pagliarini et al. 2008). The nuclear-encoded mitochondrial proteins acquire a positively charged amino-acid terminal targeting peptide, which allows them to be imported to the negatively charged mitochondrial matrix to contribute to the structure of the mitochondrion (Guarente 2008). Thus, by analogy, the nDNA contains the architect's blueprints for building a house, but the mtDNA contains the wiring diagram for energizing it (Wallace 2005; 2007).

Mitochondria harness energy by chemiosmotic coupling, which links chemical bond-forming reactions that produce ATP and membrane-transport processes; both are performed by the chain of complexes embedded in the inner membrane of mitochondria. Complexes I – IV together with the small molecules involved in the sequence of electron transfers are known as the electron-transport chain (ETC), and together with complex V (ATP synthase), compromise the machinery of oxidative phosphorylation (OXPHOS).

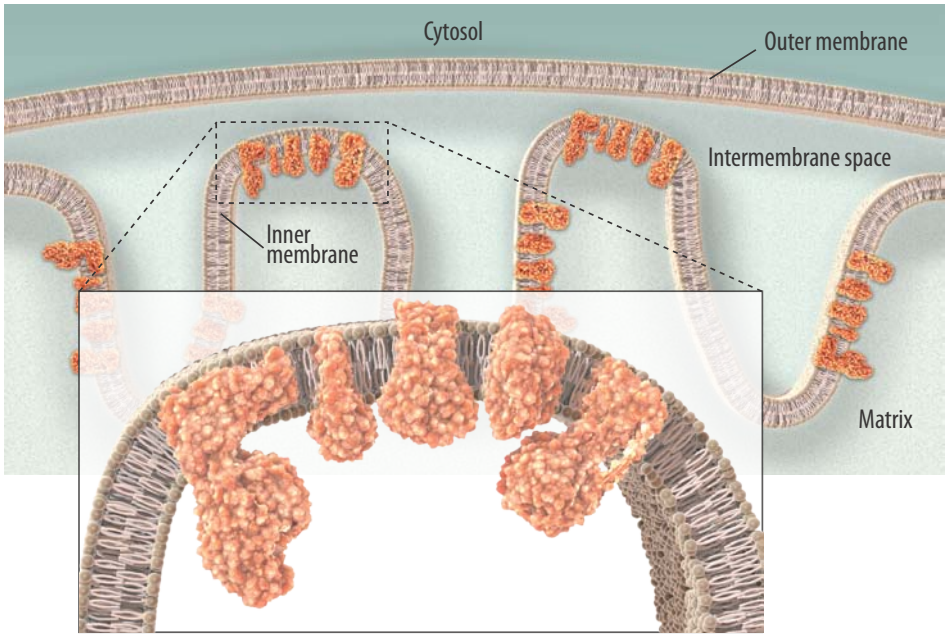

Figure 1. Mitochondrial ultrastructure and the mitochondrial respiratory chain. Schematic depicts the two lipid bi-layers that create four separate mitochondrial compartments: the mitochondrial outer membrane, the intermembrane space, the inner membrane, and the matrix. Folding of the inner membrane gives rise to cristae. The mitochondrial respiratory chain is located within the inner membrane and includes five complexes (I – V). *Modified from Ross*, JoVE, *2011 (Paper II)*.

Although mitochondria are usually depicted as static organelles, they are in fact very dynamic, mobile, and in continuous fission or fusion, with their distribution within the cell often dependent on microtubule transport (Detmer and Chan 2007; Chan 2006). Hence, their orientation and distribution varies among cell types depending upon the energy demands. For instance, mitochondria are tightly wrapped around the sperm flagellum, whereas in neurons the mitochondria appear to be more elongated, presumably for axonal transportation (Alberts 2008; 2008; Voet et al. 2012).

Regardless of their slight morphological differences, all mitochondria are structurally similar and contain two lipid bi-layers, an outer membrane and an inner membrane (Fig 1). The outer membrane contains many copies of a transport protein, *porin*, which is an aqueous channel that allows passage of proteins and molecules less than 5 kDa. The impermeable and highly convoluted inner membrane forms the *cristae*, which contain the respiratory chain (RC) complexes (complexes I – V). The number of cristae and RC complexes can vary among cell-type and tissue, presumably due to energy-demand differences (Alberts 2008; Kuznetsov et al. 2009; Kuznetsov and Margreiter 2009; Zick

et al. 2009). The impermeability of the inner membrane is most likely due to high concentrations of cardiolipin, an unusual phospholipid originally discovered in bovine cardiac muscle, and which has four fatty acids rather than the typical two (McMillin and Dowhan 2002). Due to this permeability difference, the intermembrane space is chemically equivalent to the cytosol, whereas highly selective processes determine the composition of the matrix, which contains enzymes important for pyruvate and fatty acid oxidation, such as the tricarboxylic acid (TCA) cycle, as well as enzymes required for expression of mtDNA.

Cellular respiration

The polysaccharides, lipids, and protein are broken down into smaller molecules and ATP in cells by a set of metabolic reactions and processes known as cellular respiration. Digestion breaks down the large polymeric molecules from food into monomer subunits, such as sugars from polysaccharides. These smaller molecules enter the cytosol of the cells where catabolism continues, and then move to the mitochondrion for the final steps of oxidation.

Glycolysis

An important step in cellular respiration is the breakdown of glucose to pyruvate known as glycolysis, from Greek “glyco” meaning “sweet” and “lysis” meaning “rupture”. In this ten-step process, which largely occurs in the cytosol and does not require the presence of molecular oxygen (O_2 gas), a 6-carbon glucose molecule is oxidized to form 2 molecules of the 3-carbon pyruvate. Additionally, for each molecule of glucose, 4 molecules of ATP are formed (but 2 ATP are consumed, yielding a net gain of 2 ATP) and 2 molecules of NAD^+ are reduced to form 2 NADH. For most animal cells, glycolysis is the prelude to the final stages of cellular respiration, which occurs in the matrix of mitochondria; however, for anaerobic organisms and in cases when either molecular oxygen is limited or mitochondria are dysfunctional in aerobic tissues, pyruvate can be reduced to lactate (or ethanol) so that NADH can be oxidized to NAD^+. The regeneration of NAD^+ is essential to maintain glycolysis (Guarente 2008; Alberts 2008).

Tricarboxylic acid cycle

In aerobic metabolism in animal cells, a 3-carbon pyruvate molecule is oxidized by a pyruvate dehydrogenase complex to form a 2-carbon acetyl Coenzyme A (acetyl CoA), 1 molecule of NADH, and also 1 molecule of carbon dioxide (CO_2; as waste) in the matrix of mitochondria. Acetyl CoA can also be produced from amino acids and from fatty acid metabolism via β-oxidation.

The TCA cycle, also known as the citric acid cycle or Kreb's cycle, was established in the 1930s by the seminal work done by Albert Szent-Györgyi and Hans Adolf Krebs (Wallace 2005; Alberts 2008; Wallace 2007). The TCA cycle (8 steps) accounts for approximately two-thirds of the total oxidation of carbon compounds, and 1 acetyl CoA produces 3 NADH and 1 $FADH_2$, both energy-rich activated carrier molecules, as well as 1 ATP, 1 GTP, and 2 CO_2 (as waste).

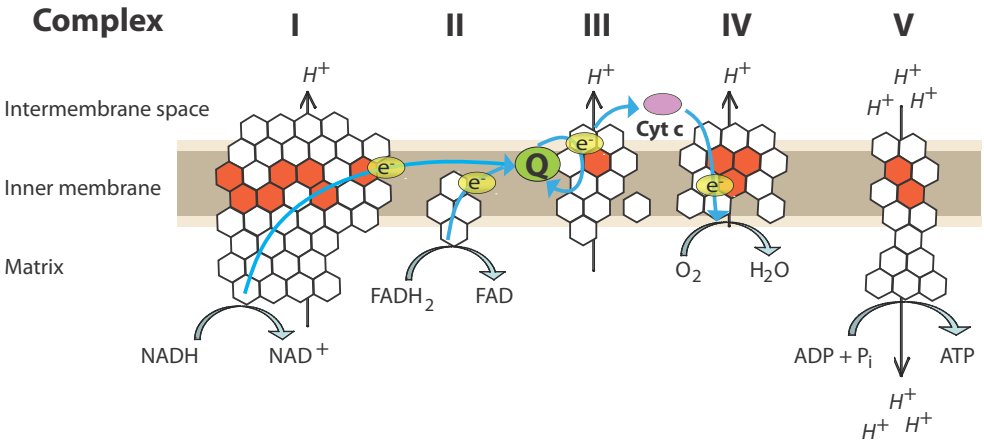

Figure 2. Mitochondrial respiratory chain complexes I-V. The five enzymes of the oxidative phosphorylation machinery are located in the inner membrane. Red hexagons represent unique subunits encoded by mtDNA, while white hexagons represent subunits encoded by nDNA. This schematic depicts the oxidation of NADH and $FADH_2$ and the flow of electrons (e^-) from complex I and II through the respiratory chain to complex IV, which creates a H^+ ions (protons) gradient across the inner membrane used by complex V (ATPase) to produce ATP.

Oxidative phosphorylation

It is in this last step of catabolism that the majority of the energy is produced, which can be used to maintain the organism's body temperature and to generate ATP. The electrons (e^-) from the high-energy carriers produced mainly from the TCA cycle, NADH and $FADH_2$, are oxidized by the ETC, which is comprised of complexes I – IV

and is embedded in the inner membrane of mitochondria (Fig 1 and 2). As the electrons (from NADH and $FADH_2$) pass along this chain of specialized electron acceptor and donor complexes (I – IV), they fall to successively lower energy states and the energy released during this process is used to pump H^+ ions (protons) across the inner membrane by complexes I, III, and IV. In doing so, an ionic gradient is created, which can be harnessed to produce ATP or dissipated to generate heat.

The ETC begins with complex I (NADH dehydrogenase), which oxidizes NADH to NAD^+ and by doing so collects 2 electrons; complex II (succinate dehydrogenase) collects 2 electrons from $FADH_2$ by conversion of succinate to fumurate in the TCA cycle. The electrons from both complexes I and II are transferred to coenzyme Q_{10} (Q) and thereby reduces Q sequentially from ubiquinone to ubiquinol. Additionally, electrons can be collected from the electron transfer flavoprotein (ETF) and ETF dehydrogenase, generated by fatty acyl-CoA dehydrogenases via the catabolism of fatty acids. The 2 electrons are transferred to complex III (bc_1 complex) and then to cytochrome *c*, which transfers them to complex IV (cytochrome *c* oxidase). Complex IV uses the 2 electrons to reduce ½ O_2 forming 1 molecule of water (H_2O). Each complex in the ETC has a greater affinity for electrons than its predecessor; thus the electrons move from a higher reducing potential to a lower reducing potential (Alberts 2008; Voet et al. 2012; Guarente 2008).

The energy released by the flow of electrons across the ETC is used to pump H^+ ions across the inner membrane. Protons are pumped across complexes I, III, and IV. This creates an electrochemical gradient, which is used to drive ATP synthesis via complex V (ATP synthase) in the critical process of oxidative phosphorylation by condensing ADP and P_i to form ATP. The newly formed ATP is exchanged for ADP across the inner membrane by adenine nucleotide translocators (ANT). The ANTs also regulate the rate of OXPHOS, which depends on the ratio between ATP and ADP/P_i. Under perfect conditions, 1 NADH molecule can produce 3 ATP, and 1 $FADH_2$ molecule can produce 2 ATP; therefore, one molecule of glucose can yield a net gain of 38 ATP by using OXPHOS (excluding the energy needed to transport ATP to the cytosol) (Alberts 2008). The OXPHOS "coupling efficiency", or the efficiency with which the electrochemical gradient is converted to ATP, can be decreased by leakage of the membrane or by uncoupling proteins (UCP). For instance, thermogenin, or UCP1, is present in brown adipose tissue and generates heat via non-shivering thermogenesis by

increasing the permeability of the inner membrane, thus allowing protons that have been pumped into the intermembrane space to return to the matrix (Nicholls et al. 1978).

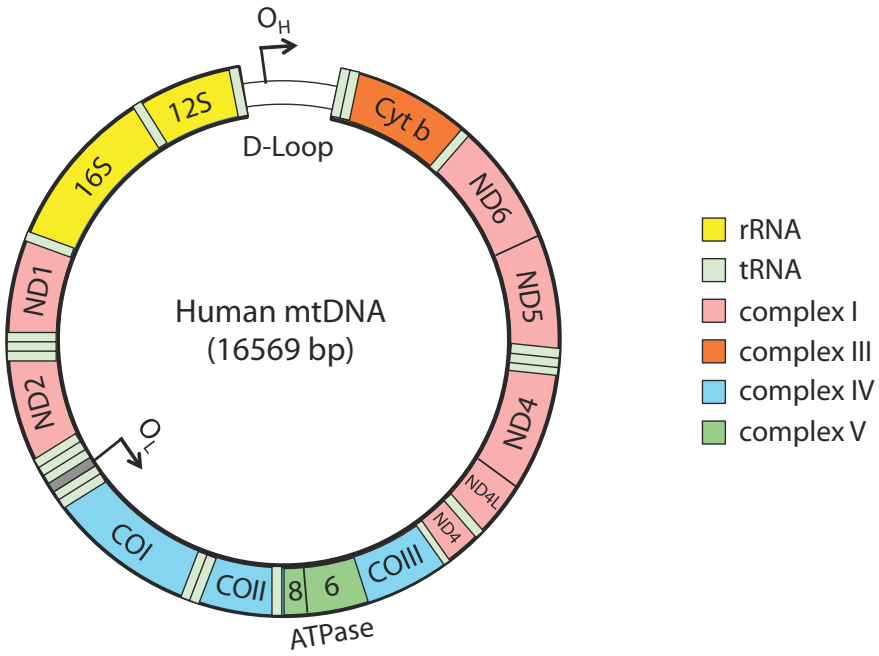

Figure 3. Mitochondrial DNA genome. Human mtDNA is a double-stranded closed circular molecule, with a G-rich heavy (H-strand) and a C-rich light (L-strand) strand, the promoters for which are contained in the non-coding D-loop region. The origin of replication of both the leading strand (O_H) and the lagging strand (O_L) are denoted. Each gene is represented by a color-encoded box. The 13 mtDNA-encoded polypeptide genes are grouped by color to indicate the corresponding OXPHOS enzyme complex.

Mitochondrial DNA

As described, mammalian mtDNA (Fig 3) contains only 37 genes that encode 13 mRNAs (all translated to RC proteins), 2 rRNAs, and 22 tRNAs. All other genetic information necessary for mitochondrial structure, and the expression and maintenance of mtDNA have been transferred to the nDNA. The inheritance of mtDNA in mammals is considered to be strictly maternal by contribution of oocyte mitochondria, with transfer of paternal inheritance of mtDNA regarded as a rare exception (Birky 2001; Giles et al. 1980; Ameur et al. 2011; Taylor et al. 2003b). The 13 mtDNA polypeptide genes encode 7 (ND1-6, ND4L) of the 45 subunits of complex I, 1 (cytochrome *b*) of the 11 subunits of complex III, 3 (COI-III) of the 13 subunits in complex IV, and 2 (ATPase 6 and 8) of the 17 subunits of complex V (ATP synthase). Complex II is entirely encoded by the nuclear genome. The mitochondrial DNA molecule has been

regarded as the smallest chromosome, and is approximately 16.5 kb in size in mammals (human: 16.6 kb; mouse: 16.3 kb). Mammalian mtDNA is a closed-circular double-stranded molecule and is present as multiple copies, normally 1,000 – 10,000 molecules per cell. The mtDNA is very compact and consists of almost exclusively encoding regions with no introns, the exception being the approximately 1 kb long displacement loop (D-loop) region, which is important for initiation of replication and transcription (Larsson 2010; Alberts 2008; Anderson et al. 1981; Larsson and Clayton 1995). Additionally, it was recently found that mtDNA molecules can form "nucleoid" structures, each approximately 100 nm in size and containing sometimes a single copy of mtDNA (Bogenhagen 2012; Kukat et al. 2011).

Replication of mitochondrial DNA

The nuclear-encoded heterotrimeric mitochondrial DNA polymerase-γ complex (POLγ or POLG) consisting of a 140 kDa catalytic α-subunit of POLγ (PolgA or Polg1, is encoded by *POLG* at chromosomal locus 15q25) and two identical 55 kDa accessory β-subunits (Polg2, encoded by *POLG2* at chromosomal locus 17q24.1). Together with the mitochondrial DNA helicase Twinkle and mitochondrial single-stranded DNA-binding protein (mtSSB) form the mitochondrial replication machinery (Longley et al. 1998; Korhonen et al. 2004; Stumpf and Copeland 2011). The mtDNA polymerase has an important role in both replication and repair of the mtDNA, with the catalytic subunit (PolgA) performing three key enzymatic activities: (i) DNA polymerase activity, (ii) 3'-5' exonuclease activity that proofreads misincorporated nucleotides, and (iii) 5'-dRP lyase activity required for base excision repair (Graziewicz et al. 2006; Kaguni 2004). The catalytic subunit of PolgA has three highly conserved exonuclease motifs at the N-terminal (Exo 1-3), with conserved aspartate and glutamate residues (Bernad et al. 1989; Longley et al. 2001). Mutations in the proof-reading regions of PolgA can lead to impaired mtDNA which can result in dysfunction of the mitochondrial respiratory chain (Stumpf and Copeland 2011; Hudson and Chinnery 2006).

Reactive oxygen species

Mitochondria naturally generate reactive oxygen species (ROS) as an important by-product of oxidative phosphorylation. ROS production occurs when an electron escapes the ETC or when an electron carrier harbors excess electrons, and then reacts with O_2 to

generate a superoxide anion ($O_2^{\bullet-}$). Mitochondrial superoxide dismutase enzymes (SOD: MnSOD, Cu/ZnSOD) located in the matrix, intermembrane, and cytosol, can convert superoxide $O_2^{\bullet-}$ to hydrogen peroxide (H_2O_2), which can then diffuse out of the mitochondria and be reduced to water by peroxisomal catalase or glutathione peroxidase (GPx1). However, H_2O_2 can also react with transition metals and be converted to a highly reactive hydroxyl radical ($^{\bullet}OH$). The three forms of ROS ($O_2^{\bullet-}$, H_2O_2, $^{\bullet}OH$) are mainly produced by complex I and III. ROS formation can be regulated by physiological factors, including the mitochondrial membrane potential, intracellular calcium (Ca^{2+}), and nitric oxide (NO) (Zhang and Gutterman 2007). Elevated ROS can cause damage to DNA, proteins, and lipids, can contribute to mitochondrial damage in a range of pathologies, and have also been implicated in the development and maintenance of the metabolic syndrome (James et al. 2012; Murphy 2009; Dröge 2002). However, ROS may also have positive effects on other aspects of physiology by retrograde redox signaling from the mitochondria to the rest of the cell (Shlomai 2010; Dröge 2002).

Mitochondrial DNA mutations

Mammalian mtDNA replication takes place in the mitochondrial matrix, is under relaxed control, and is independent of cell cycle (Bogenhagen and Clayton 1977). The mutation rates of mtDNA is very high, approximately 10-fold higher than in nDNA (Brown et al. 1979; Guarente 2008). Furthermore, since mtDNA has no introns or non-coding sequences, a mutation is likely to affect gene function. Impaired mtDNA can be the result of point mutations, deletions, or duplications, and can be deleterious, beneficial, or neutral. The mitochondrial genome continues to replicate in mitotic and meiotic cells; therefore, mtDNA mutations can be transmitted through the maternal germline (Ameur et al. 2011; Guarente 2008). Point mutations are most often maternally transmitted in highly variable amounts (Brown et al. 2001), while the deletions are considered sporadic, with the most deleterious mtDNA mutations eliminated via a strong purifying selection in combination with a "genetic bottleneck" for mtDNA transmission (Stewart et al. 2008); however, the mechanism underlying the purifying selection remains unclear. Additionally, mtDNA and mitochondria are turned over in post-mitotic cells, which can contribute to clonal expansion of the mutant mtDNA over time.

More than one species of mtDNA can be found in individual cells, a state known as heteroplasmy. When a heteroplasmic cell divides the distribution of wild-type and mutant mtDNA into the daughter cells is random; this can ultimately lead to segregation of the wild-type and mutant mtDNA, referred to as homoplasmy (Larsson and Clayton 1995). Moreover, mtDNA mutations can disrupt mitochondrial function if the percentage of mutant mtDNA per cell reaches a threshold where inadequate functional mitochondria remain unable to perform sufficient OXPHOS. Thus, effective and faithful mtDNA replication is essential for cellular homeostasis and survival.

Mitochondrial disease

Deleterious mutations affecting mitochondrial function can arise from either mtDNA and/or nDNA genes that encode for mitochondrial components, including structural proteins involved in mitochondrial energy metabolism and maintenance of the mtDNA, such as POLγ. Such mutations may either be inherited or can be formed *de novo* (Wallace 1999; Larsson and Clayton 1995; Smeitink et al. 2001). Thus, mitochondrial disease is not a single entity, but rather a large heterogeneous group of "inborn" or *de novo* acquired errors of metabolism caused by genetically based OXPHOS dysfunction. The incidence of mitochondrial disease is estimated to be 1 in 8,500 newborn children (Chinnery and Turnbull 2001) which, in the United States alone, translates into 3,700 new cases every year. There is pronounced variability in the presentation of mitochondrial disease which complicates its clinical diagnosis; presentation may vary from infancy into adulthood. The onset is usually progressive and multi-systemic with organs with high-energy demands typically affected, including the CNS, cardiac and skeletal muscle, retina, kidney, as well as bone marrow (Haas et al. 2007). Early onset typically correlates with more severe disease. Diagnosis can be difficult due to nonspecific presentation of the disorders and also due to the lack of reliable and specific biomarkers (Haas et al. 2007).

Fifty years ago, the first known case of a mitochondrial disorder was diagnosed (Luft et al. 1962), even before the existence of mtDNA was reported in 1963-1964 (Nass and Nass 1963; Luck and Reich 1964; Schatz et al. 1964). Today, a large number of disorders have been described and the list continues to grow, with more than 229

pathogenic base-substitution mutations identified (see MITOMAP website) (Ruiz-Pesini et al. 2007; Wallace 2005). The most common childhood-onset is Leigh syndrome, a progressive neurodegenerative disorder that involves developmental regression, brainstem dysfunction, and lactic acidosis, caused by either mtDNA and nDNA mutations (Castro-Gago et al. 2006). Leber's hereditary optic neuropathy (LHON) is the most common mtDNA disorder that typically presents in adult males with sub-acute bilateral visual failure; it is typically caused by point mutations affecting complex I (G11778A in ND4, G3460A in ND1, T14484C in ND6) (Howell 1997; Chinnery et al. 2000). Approximately 150 mutations have bee identified in the human *POLG* in patients with mitochondrial diseases, and contributes to several disorders including progressive external ophthalmoplegia (PEO) and Alpers syndrome (Stumpf and Copeland 2011). Mitochondrial diseases are associated with chronic morbidity and are often fatal; thus, although the current management of patients with these disorders is largely supportive, the past twenty years has provided insights into the pathophysiology of mitochondrial disease.

AGEING

The remarkable 30-year increase in life expectancy during the last century is a great achievement. It is estimated that most newborns will survive until at least 75 years of age (Christensen et al. 2009). As the average age of the western world population is increasing, countries are predicting significant demographic changes over the next two-to-three decades. In the United States, the older population, defined as persons 65 years or more, is expected to grow to be 19% of the population, an approximate 7% increase since the year 2000 (see Administration on Aging: www.aoa.gov). Also Sweden is facing significant changes, with a projected increase to 30% of the aged population by 2030 (see Sweden.se). Although these are projections, the increasing proportions of older individuals constitute a challenge in the western world. Research efforts to increase the health of this group by novel treatments of age-related disorders, and in particular neurodegenerative diseases affecting the brain, such as Alzheimer's disease and forms of dementia, Parkinson's disease, and stroke are needed. Moreover, there is a need to better understand the underlying mechanisms of the ageing process itself (Christensen et al. 2009) to be able to counteract some of its effects and maintain health of the older population.

What is ageing *per se*?

What exactly is *ageing*? Perhaps ironically, ageing is arguably the most familiar of all the biological processes, yet it is the least defined and understood. While there are many descriptions as to what happens as an organism "ages", less is known about what regulates this process. Ageing is a complex process affecting virtually all vital parameters of an organism, characterized by an overall decrease in many cellular functions that lead to increasing risk of disease and death. The ageing process is often accompanied by a decline in fertility, cellular senescence, loss of tissue homeostasis, and decline in organ function, which can lead to less adaptability to stress stimuli and increased morbidity. The difficulty in understanding the cause-effect relationship between different chronological events during ageing is perhaps due to the interdependence of many biological processes, which makes it experimentally difficult to isolate only one possible system or pathway.

Interestingly, the ageing process varies among species, and even among individuals within the same species. There is even variability among tissues, with dividing cells more influenced by telomere erosion, gene mutation, and epigenetic dysregulation. In postmitotic cells, protein aggregation and mitochondrial dysfunction may be more important, with oxidative stress possibly affecting both intracellular moieties (Kirkwood 2010). Variability can even be found among cell types; *e.g.* fibroblasts grown in culture undergo "cellular senescence", compared with immortal malignantly transformed cells (Kirkwood 2005b).

Theories on ageing

Some of the major hypotheses of ageing that emerged over the last 60 years will be presented here in an attempt to illustrate the depth and breadth of the complex field of ageing, from evolutionary theories to programmed ageing theories, including the "Mitochondrial Theory of Aging", which is the main focus of this thesis.

Evolutionary views

One of the first modern theories of ageing, "Mutation Accumulation", was proposed by Sir Peter Medawar in 1952 (Medawar 1952). Essentially, individuals in the wild rarely survived to advanced ages, and they were therefore not able to provide much help towards the survival of younger, more fertile individuals. This minimized evolutionary mechanisms to improve the conditions of aged individuals. Hence, the accumulation of random, detrimental mutations would not be eliminated by natural selection and would therefore lead to declining viability and/or fertility with ages. While this seems plausible, the regulation of gene expression, including cellular senescence, and the evidence that genes which can cause ageing in fact may not undergo random mutations, may present limitations to Medawar's theory (Guarente and Kenyon 2000).

George Williams further developed Medawar's theory in 1957 (Williams 1957) with the "Antagonistic Pleiotropy Hypothesis" as an explanation for senescence. Williams suggested that a gene(s) beneficial for reproduction early in life could have been naturally selected even if the effects of this gene(s) later in life might have been detrimental to the organism's fitness. For instance high levels of hormones, such as testosterone and estrogen, lead to increased fitness in early life and cause decreased

fitness in later life due to a higher risk for cancers (Gann et al. 1996). While this theory seems plausible, it has been shown in drosophila selected for longevity, that long-lived, inbred flies actually are more fertile than short-lived flies (Rose and Graves 1989).

The "Disposable Soma theory" was proposed in 1977 by Thomas Kirkwood and suggested that the body must budget the amount of energy available for all of its processes, including metabolism, reproduction, repair, and maintenance, given a finite amount of food resources (Kirkwood 1977). While this theory is intuitive, there is accumulating evidence that, in fact, caloric restriction increases longevity and lifetime reproductive fitness (Weindruch 1996; Masoro 2005).

Is ageing programmed?

Ageing theories may also encompass mechanisms, such as apoptosis, cellular senescence, and death of specific individuals in a population if such death is advantageous for the survial of the species. In this context, one might ask why there are end artery systems in both heart and the brain. Examples of a limited lifespan include semelparous organisms, *e.g.* pacific salmon (*Oncorhynchus*), in which death comes suddenly after spawning. Such examples have contributed to the development of programmed ageing theories (Lamberts et al. 1997; Kirkwood 2005b; Weismann 1889).

Several theories propose that ageing is the result of progressive random accumulation of damage and/or mutations. Such damage would cause changes in cellular homeostasis and functions essential for cell survival, including mechanisms for the maintanence and/or repair of DNA and proteins (Kirkwood and Austad 2000). One such hypothesis is based on observations by Leonard Hayflick and Paul Moorhead in 1961 (Hayflick and Moorhead 1961), who discovered that normal diploid cells lose the ability to divide after approximately 50 times. This phenomenon, known as "cellular senescence" or the "Hayflick limit", disproved the immortality theory of Alexis Carrel (Carrel and Ebeling 1921). Carrel's observations were likely due to a technical error, in which he inadvertently added cells to the culture of chick embryonic stem cells on a daily basis; the "Hayflick limit" has been replicated and is now a pillar of biology.

In fact, cellular senescence has been found to correlate with the length of telomeres (Yu et al. 1990), a repeated genetic code on the end region of nDNA that is shortened after each replication. Once the telomeres are depleted, the cell can no longer divide and will thus become senescent. Stem cells use telomerase to restore telomere length; however, it has been shown that telomerase cannot completely prevent telomere shortening, thus providing a putative mechanism for the temporal limit of stem cell replication with age (Flores et al. 2005). The amount of senescent cells has been found to increase with age (Rodier and Campisi 2011). While there is some evidence that cellular senescence promotes protection against cancer (Collado et al. 2007; Collado and Serrano 2010), there is increasing evidence demonstrating that senescent cells secrete pro-inflammatory cytokines (Wolf et al. 2012), which may contribute to the onset and progression of many age-related disorders, including Alzheimer's disease and forms of dementia, as well as osteoarthritis and pain (Sardi et al. 2011; Anderson and Loeser 2010).

In contrary to theories of programmed ageing, many studies have indicated that genetic background can predict lifespan (Piper et al. 2008; Klass 1983; Larsson 2010; Kenyon 2010). More recently, this has been expanded to include lifestyle factors, such as diet, caloric intake, exercise, as well as epigenetics, which may modulate the ageing process (Sadler et al. 2011; Kirkwood 2005a; Rando and Chang 2012; Winnefeld and Lyko 2012; Rowe and Kahn 1987; Hubert et al. 2002).

Mitochondria and ageing

With the discovery of ROS as by-products of normal respiration of the electron transport chain, and given the proximity of the mtDNA to the inner membrane where oxidants are formed, came the hypothesis that oxidative stress and mitochondria function could play a pivotal role in the ageing progress. In 1956, Denham Harman (Harman 1956) proposed the "Free-radical Theory of Aging" (FRTA), which suggests that ROS drive ageing by creating damage to cellular structures and processes which accumulate over time. This theory was later revised to implicate mitochondria as the main source of ROS production, renaming FRTA the "Mitochondrial Theory of Aging" (Harman 1972). The theory predicts that a "vicious cycle" links ROS production to the ageing process by (i) accumulation of mitochondrial DNA damage, (ii) progressive respiratory chain dysfunction, and (iii) increased ROS production. Thus, this theory

suggests that damage to mtDNA slowly accumulates with time and causes ageing phenotypes by interfering with bioenergetic homeostasis or by producing loss of cells because of apoptosis or cellular senescence (Harman 1972; Wallace 1999).

The "Mitochondrial Theory of Aging" is supported by a wealth of correlative data, but has remained controversial in the absence of experimental data. High levels of certain mtDNA mutations impair respiratory chain function and cause a plethora of human diseases (Smeitink et al. 2001; Wallace 1999; Larsson and Clayton 1995). It has been extensively documented that the normal ageing process in humans (Corral-Debrinski et al. 1992; Soong et al. 1992; Cortopassi and Arnheim 1990), monkeys (Schwarze et al. 1995), and rodents (Khaidakov et al. 2003; Tanhauser and Laipis 1995) is associated with accumulation of mtDNA point mutations and deletions. There are also reports showing that high levels of specific mtDNA point mutations in the non-coding control regions of mtDNA are associated with longevity (Michikawa et al. 1999).

The role of mitochondrial mutations in ageing has been questioned because the overall level of mtDNA mutations is usually lower than the threshold needed to cause respiratory chain dysfunction (Cottrell and Turnbull 2000; Larsson and Oldfors 2001). However, somatic mtDNA mutations associated with ageing are not evenly distributed and can accumulate clonally in certain cells where they can cause RC deficiency (Larsson and Oldfors 2001; Larsson 2010; Fayet et al. 2002; Kraytsberg et al. 2006). This leads to a mosaic pattern with scattered RC deficient cells in different tissues such as heart (Müller-Höcker 1989), brain (Cottrell et al. 2001; 2002; Bender et al. 2006), and skeletal muscle (Taylor et al. 2003a; Müller-Höcker 1990; Brierley et al. 1998) of aged individuals. In cells with RC deficiencies, there is an accumulation of point mutations or deletions (Fayet et al. 2002; Kraytsberg et al. 2006). Furthermore, it is well established that, with age, the number of mitochondria decreases as does mitochondrial structural integrity, manifested as matrix vacuolization, swelling and enlargement, carbonylated proteins, cristae abnormalities, and intra-mitochondrial paracrystalline inclusions (Yasuda et al. 2006; Frenzel and Feimann 1984; Wilson and Franks 1975; Samorajski et al. 1971; Herbener 1976). Lastly, it has been found that somatic mtDNA mutations accumulate in all animal tissues, and do so at a rate relative to the ageing rate of the specific species (Wallace 2005).

The mtDNA mutator mouse

To experimentally address the "Mitochondrial Theory of Aging", the present work takes advantage of a homozygous knock-in mouse (mtDNA mutator mouse; Fig 4) expressing a proof-reading deficient version of the nucleus-encoded catalytic subunit of mtDNA polymerase-γ (PolgA), created by our collaborators at Karolinska Institutet (Trifunovic et al. 2004). In these mtDNA mutator mice, the wild-type mtDNA PolgA gene was replaced with a PolgA in which the proof-reading exonuclease function was inactivated by an amino acid substitution (D257A). Other studies have shown that mutations in the catalytic aspartates disrupt exonuclease activity and result in a 20-fold increase *in vitro* and a 500-fold increase *in vivo* in mtDNA base substitutions (reviewed in Stumpf and Copeland 2011). The mtDNA mutator mice ($PolgA^{mut/mut}$) develop high levels of point mutations (20-30 mutations per mtDNA molecule) and linear deletions (~25% of total mtDNA), which begin during midgestation and increase throughout the lives of the animals. The model demonstrates a cause and effect relationship between increasing somatic mtDNA mutation levels and several phenotypes associated with ageing that are manifested much earlier in life.

Figure 4. A mtDNA mutator mouse at 45 weeks showing progeroid ageing phenotypes, including canities (graying of hair), alopecia (hair loss), kyphosis (curvature of the spine), elongation of ears, reduction in body size, and weight loss.

The homozygous mtDNA mutator mice show multiple signs of human-like ageing occurring prematurely, with an onset of visible phenotypes occurring already after 20-24 weeks of age. The lifespan is greatly reduced, from 2.5-3 years to 42-45 weeks. Additionally, mtDNA mutator mice also develop weight loss, canities (graying of hair), alopecia (hair loss), anemia, kyphosis (curvature of the spine), osteoporosis, sarcopenia (skeletal muscle loss), loss of subcutaneous fat, reduced fertility, and hearing loss (Trifunovic et al. 2004; Niu et al. 2007). A premature ageing phenotype has also been reported in mice generated elsewhere using a similar strategy (Kujoth et al. 2005).

Interestingly, studies on peripheral tissues from mtDNA mutator mice did not find an increase in ROS production (Trifunovic et al. 2005; Kujoth et al. 2005; Loeb et al. 2005), suggesting respiratory chain dysfunction *per se* rather than ROS accumulation may be causing the premature ageing phenotypes. Although the RC subunits are synthesized at normal rates, it was found that the RC complexes are not stable, which may explain the decreased respiration with lack of increased ROS production (Edgar et al. 2009). This decrease in stability could be due to amino acid substitutions as a result of mtDNA point mutations, which could impair the assembly and stability of the RC (Edgar et al. 2009).

Thus, there are both observational and experimental data to support the "Mitochondrial Theory of Aging", in that mitochondrial dysfunction may be an important mechanism in ageing. However, a critical question that had yet to be tested is if progeroid ageing is also seen in the brains of these animals. Furthermore, the downstream effects of impaired oxidative phosphorylation and its implication on the ageing process in the brain remained unclear. Studies on the brain of mtDNA mutator mice are a major focus of this thesis.

AIMS OF THE THESIS

The overall goal was to investigate how elevated somatic mtDNA mutations may translate to age-related functional changes in the central nervous system, using a transgenic mouse model of premature ageing, the mtDNA mutator mouse.

Specifically, the aims addressed in this thesis were to:

Investigate if the accumulation of mtDNA mutations would lead to progressive mitochondrial respiratory chain dysfunction

Study the down-stream metabolic effects of reduced cellular respiration on the ageing process

Determine if the premature ageing phenotypes of the mtDNA mutator mouse, as a consequence of elevated mtDNA mutations and mitochondrial dysfunction, are paralleled in *normal* ageing

Identify therapies to combat mitochondrial deficiencies and test if the premature ageing phenotypes in mtDNA mutator mice can be rescued

Investigate the possible consequences of mtDNA mutations and mitochondrial dysfunction for brain development

MATERIALS AND METHODS

ANIMALS

Experiments were approved by the Animal Ethics Committee of the Northern Stockholm region and conducted in accordance with international animal welfare standards. Adequate measures were taken to minimize pain and discomfort.

The mtDNA mutator mouse

Prematurely ageing mtDNA mutator mice ($PolgA^{mut/mut}$), heterozygotes ($PolgA^{mut/WT}$), and wild-type control littermates ($PolgA^{WT/WT}$) were obtained by intercrossing heterozygous mice and genotyping by PCR (forward: 5'-GCCATCTCACCAGCCC GTAT-3'; reverse: 5'-GTGAGGAGAGTGGCCGCTAA-3') (Trifunovic et al. 2004). Mice heterozygous for the mutator allele ($PolgA^{mut/WT}$) were backcrossed to C57Bl/6J mice for at least 5 generations.

In Paper III, C57BL/6J mice were used for backcrossing to create different "lines" of mtDNA mutator mice (Fig 5). In Line 1, heterozygotes were intercrossed for several (F>10) generations to obtain mtDNA mutator mice. In Line 2, male heterozygotes were crossed (F>4) with wild-type female C57Bl/6J mice to reintroduce wild-type mtDNA and nDNA. Wild-type nDNA alone was reintroduced by crossing (F>4) female heterozygotes with wild-type male C57Bl/6J mice in Line 3.

In Paper I, control strains C57Bl/6J and 129/SvImJ mice (JAX Mice Strains) were also studied to verify that the results obtained by both ^{1}H-MRS and HPLC were not due to the mixed background of the mtDNA mutator mice.

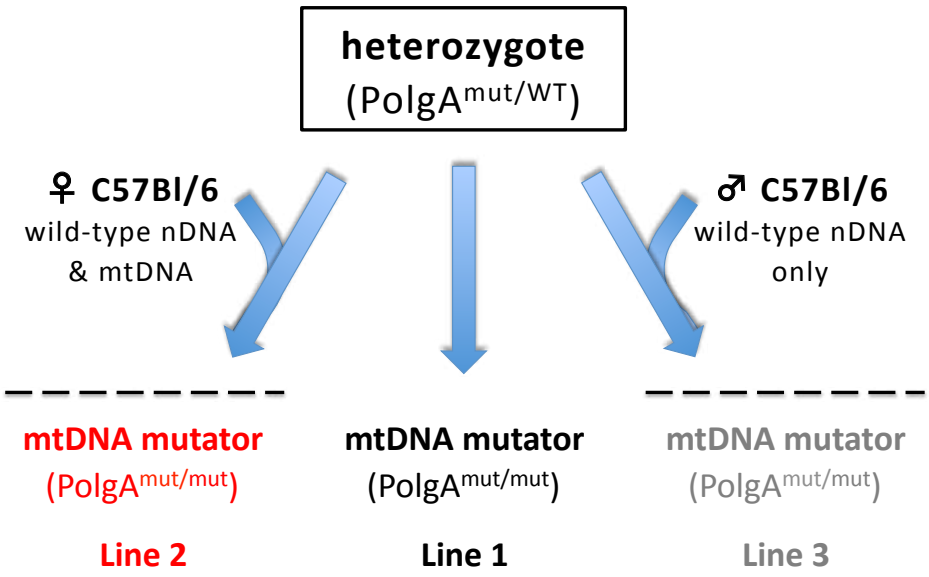

Figure 5. Breeding schemes in mtDNA mutator mice. In Line 1, heterozygotes (PolgA$^{mut/WT}$) were intercrossed for several (F>10) generations to obtain mtDNA mutator mice (PolgA$^{mut/mut}$). In Line 2, male heterozygotes were crossed (F>4) with wild-type C57Bl/6 females to introduce wild-type mtDNA and wild-type nuclear DNA (nDNA). Wild-type nDNA alone was reintroduced by crossing (F>4) female heterozygotes with wild-type C57Bl/6 males in Line 3. The dashed lines indicate that after crossing with wild-type C57Bl/6 mice the heterozygous offspring are then intercrossed to obtain mtDNA mutator mice.

Housing and diet

Mice were group-housed (no more than 5 animals per cage) based on sex in an enriched environment, had access to food (R70 or R34; Lactamin/Lantmännen, Stockholm, Sweden) and water *ad libitum*, and were kept on a 12:12 h light:dark cycle (lights on at 6.00) at 22-23°C and 60% humidity.

In Paper IV, mice were group-housed (no more than 4 animals per cage) based also on genotype, and received a standard diet (R34; Lactamin/Lantmännen) until 20 weeks of age. After 20 weeks of age, mtDNA mutator and wild-type mice were fed either a control diet (NIH-31 Rodent Diet, Harlan Teklad Diets, Madison, WI, USA) or the same control diet supplemented with NT-020 plus BioVin® (NT-020-BV) (135 mg kg^{-1}; NaturaTherapeutics, Inc. supplied the supplement to Harlan Teklad). NT-020-BV contains green tea, blueberry, carnosine, vitamin D_3, and grape extract. Food consumption, weight changes, and visible ageing phenotypes were recorded on a weekly basis.

IN VIVO TECHNIQUES

Magnetic resonance imaging

Animal preparation

In Papers I and III, animals were anesthetized with 3.5% isoflurane for induction and 2.0% for maintenance with 30% oxygen. Mice were attached to an acrylic rig in a supine position and placed inside the magnet (Fig 6). Body temperature was maintained at 36 ± 0.5 °C with a warm laminar air stream. Heart rate and respiration were monitored, and the percentage of isoflurane was regulated to maintain 80 ± 20 respirations min^{-1}.

Figure 6. BioSpec MRI system. Example of a MRI scanner for small animal research used at Karolinska Institutet (Papers I and III). *Photo courtesy of Bruker Corporation.*

Inversion recovery imaging

In Paper III, MRI was performed on animals as using a horizontal 4.7 B 40 cm^{-1} magnet (BioSpec Avance 47/40; Bruker, Ettlingen, Germany), fitted with a 12-cm inner diameter self-shielded gradient system (maximum gradient strength = 200 mB m^{-1}). A linear birdcage resonator with an inner diameter of 25 mm was used for excitation and detection. The scanner was controlled by a Linux workstation and appropriate software (Paravision 3.0.1; Bruker). The sequence used for inversion

recovery imaging had the following parameters: echo time (TE) 35.6 ms, repetition time (TR) 2566.8 ms, rapid acquisition with relaxation enhancement (RARE)-factor 8 with RARE-maximum 4, inversion time 450 ms, and matrix size 64 x 64 x 128 with 2 averages. The field of view (FOV) was 0.9 x 1.2 (or 1.4 for larger voxel) x 1.8 cm, yielding the following directional resolutions: 0.14 mm (dorso-lateral), 0.18 mm (left-right), and 0.14 mm (rostro-caudal).

^{1}H-Magnetic resonance spectroscopy

In Paper I, ^{1}H-MRS was performed on animals utilizing the same MR equipment that was described above for inversion recovery imaging. Because lactate is mainly affected by chemical shift displacement in the ^{1}H spectrum, minimization of possible spectrum contamination from lipids and macromolecules becomes critical for accurate lactate quantification. Voxel shape and localization was achieved by point-resolved spectroscopy (PRESS) using Hermite radio frequency (RF) pulses with a matched bandwidth (BW) of 5 kHz. To enhance voxel shape definition, outer volume suppression (OVS) was applied using hyperbolic secant pulses with a BW of 20 kHz. As a result, the maximum voxel displacement referenced to lactate was about 10% of the voxel size. The quality of the spectra was further improved by phase cycling of the RF pulses and the receiver in 16 steps (exorcycle), thus reducing the contribution of unwanted signals arising from nonrefocused coherencies. The chosen short TE of 15.9 ms delivers high signal-to-noise ratio (SNR) and does not complicate the spectrum by the development of j-coupled (indirect dipole–dipole coupling) spin–spin systems of lactate. To achieve sufficient accuracy for quantification, a TR of sufficient length (3,500 ms) was chosen, allowing complete relaxation of most metabolites in the spectrum between consecutive scans. Reliable water suppression was accomplished by applying the variable power RF pulses and optimized relaxation delays (VAPOR) method (Tkáč et al. 1999) in three steps. Total length of the water suppression module interleaved with OVS was 700 ms, allowing sufficient water suppression during the time of data acquisition.

Spectra from cerebral cortex and striatum were obtained from volumes of interest (VOI) of 10.2 and 20.0 μL, respectively, with 512 averages and a spectral width of 2 kHz. This resulted in an average SNR of 5 (cerebral cortex) and 10 (striatum) in reference to the creatine peak at 3.03 ppm. The spectral resolution was improved by

local shimming at VOI, resulting in a full width at one-half maximum of the water peak of 8–13 Hz. The accurate positioning of the VOI was based on multislice high-resolution anatomical images (fast spin echo/RARE) in axial, sagittal, and coronal planes. The required contrast was achieved by T1/T2 weighting with the following parameters: TR/TE = 2,500/47 ms (echo spacing = 11.7 ms and number of echoes = 8), pixel size = 0.12 x 0.12 mm^2, and slice thickness = 1 mm. In the axial position, the slice package was positioned with the first slice at the rhinal fissure. The VOI in cerebral cortex (4.0 x 1.6 x 1.6 mm = 10.2 μL) was positioned as illustrated in Figure 7, taking care not to include the subdural space. In striatum, the VOI (5.0 x 2.0 x 2.0 mm = 20.0 μL) was positioned 9.0 mm caudal to the rhinal fissure.

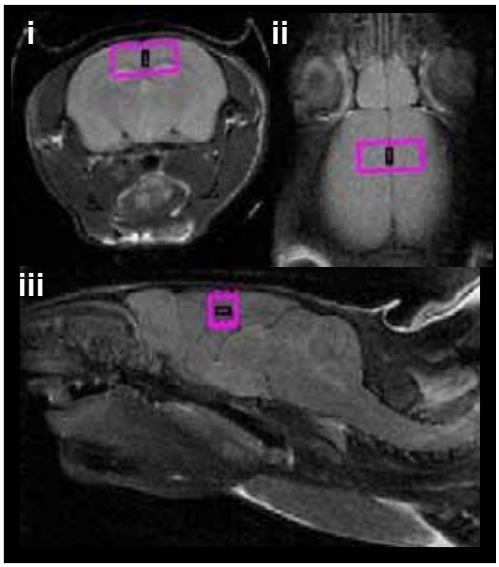

Figure 7. Volume of interest (VOI) for ^{1}H-MRS. Position of the VOI in cerebral cortex in (i) axial, (ii) coronal, and (iii) sagittal planes. *Modified from Ross* et al., PNAS, *2010 (Paper I).*

The software package LCModel (http://sprovencher.com) was used for analysis of the spectra (Provencher 1993; 2001), and statistics were applied as previously described (Öberg et al. 2008). The quantification algorithm of LCModel applies linear combinations of model spectra to calculate the best fit of the experimental spectrum. The model spectra are calibrated to match magnetic field strength, sequence type, and sequence parameters used for data acquisition. Lactate concentrations were calculated as ratios to the total creatine concentrations (Cr + PCr). Criteria for reliable metabolite quantification were based on the Cramér–Rao lower bounds (CRLB) for each metabolite as well as the CRLB for sum of spectrally overlapping metabolites, which estimates the SD of how the model spectra fit the experimental data. Metabolites with CRLB less than 50% were considered for further analysis. This methodology has been used by others (Ackl et al. 2005; Frederick et al. 2004).

Locomotion

In Paper IV, spontaneous locomotor activity in an open-field (Fig 8) was studied in mtDNA mutator and wild-type mice using a multi-cage infrared-sensitive motion detection system (AccuScan Instruments, Columbus, OH, USA). Total distance and rearing were recorded at 5-min intervals over 90 min. Total distance traveled (horizontal activity) was recorded in centimeters and rearing (vertical activity) was determined by vertical sensor beam-breaks using appropriate software (VersaMax Activity Monitor; AccuScan Instruments). Transparent locomotor chambers (40 x 40 x 30 cm) were equipped with a grid of infrared beams at floor level and 7.5 cm above. Wooden shavings were placed on the floor of the boxes prior to testing. Animals were habituated in a dimly lit, low-noise, and ventilated experimental room kept at 20-22 °C for 1 hour prior to testing. Experiments were performed between 12.00 and 17.00 (light phase), and the locomotor boxes were cleaned with 70% ethanol after each test period.

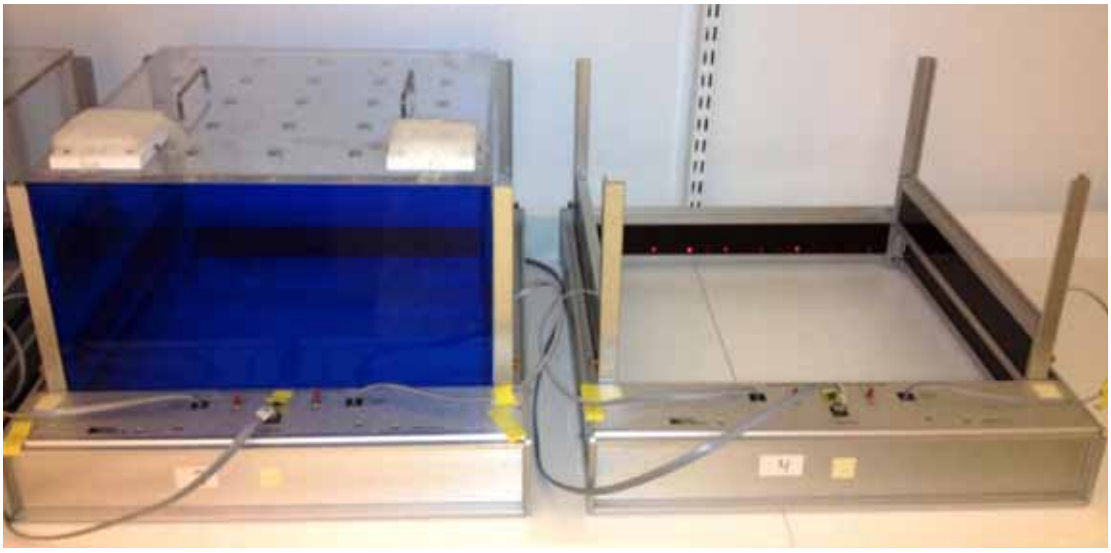

Figure 8. Open-field activity boxes. Spontaneous locomotor activity in mice was monitored at 5-minute intervals over 90 minutes using an infrared-sensitive motion detection system (Paper IV).

Gait analysis

In Paper IV, dynamic and static gait parameters, as well as spatial and temporal aspects of inter-limb coordination were recorded (CatWalk™ XT System; Noldus Information Technology, Wageningen, The Netherlands) in mtDNA mutator and wild-type mice. This technique has been used to assess impaired gait after injury and in disease

(Hamers et al. 2006; Wang et al. 2008; Kopecky et al. 2012; Chuang et al. 2010; Vrinten and Hamers 2003). The apparatus consists of a glass walkway encased with a fluorescent light (Fig 9). The footprints of the animals are illuminated as they walk down the glass platform such that the luminescence is proportional to the pressure intensity. Animals are allowed to walk freely down the 90 x 10 cm corridor. A camera mounted underneath the walkway captures a 20 x 10 cm field. A "run" is initiated by the software when a mouse enters into the field of view, and if the mouse exits the field of view within 7 seconds and has a less than 60% variation in speed, the run is considered to be "compliant". If a mouse does not satisfactorily cross the field of view (*e.g.* stops for an extended period of time, changes direction), the run is considered to be "non-compliant". If a mouse does not move once placed on the walkway, the run was defined to be "non-mobile". Three to five runs were recorded for each animal at each time point and parameters from the compliant runs were analyzed (CatWalk™ software). The walkway was cleaned with 70% ethanol between animals. Experiments were performed between 12.00 and 17.00 (light phase) in a dimly lit, low-noise, and ventilated experimental room kept at 20-22 °C.

Figure 9. Gait analysis. Unforced locomotion was recorded as mice walked down the walkway, and dynamic and static gait parameters were analyzed (Paper IV). *Photo courtesy of Noldus Information Technology.*

Videography

Homozygous mtDNA mutator and wild-type mice were filmed (Canon HG10, Canon USA Inc.) and movies were created using appropriate software (Mac iMovie '09, v.8.0.6; Apple Inc., USA).

HISTOCHEMICAL-BASED TECHNIQUES

Tissue preparation for cryosectioning

For preparation of fresh frozen sections for histochemistry and *in situ* hybridization (Papers I – III), animals were killed by cervical dislocation; tissues (brain, liver, heart) were rapidly frozen on dry ice and stored at −80 °C. Frozen tissues were embedded (Tissue-Tek; Sakura Finetek USA, Inc, Torrance, CA, USA), and 14-µm cryostat (Microm Model HM-500 M Cryostat; Microm, Walldorf, Germany) sections taken at −21 °C, were thawed onto slides (Super Frost; Menzel-Gläser, Braunschweig, Germany) and stored at −20 °C until use.

Histology

For Paper III, slides were stained with either 0.5% cresyl violet or hematoxylin and eosin, dehydrated in increasing concentrations of ethanol (70%, 95%, and 99.5%), mounted (Entellan; VWR International, West Chester, Pennsylvania, PA, USA), and coverslipped.

Immunohistochemistry

For Paper III, sections were blocked with 1% horse serum and 0.3% Triton-X in 0.1M PBS, pH 7.0 for 24 h at room temperature (RT), immunolabeled for glial fibrillary acidic protein (anti-GFAP produced in rabbit, 1:100 in blocking solution; Sigma, St. Louis, MO, USA) for 24 h at 4°C. Secondary antibodies (Goat Anti-Rabbit IgG (H+L) conjugated with Cyanine Cy3, 1:400 in blocking solution; Jackson ImmunoResearch, West Grove, PA, USA) were applied for 1 h at RT. Slides were washed, mounted

(Veactashield® Mounting Medium; Vector Laboratories, Burlingame, CA, USA), and coverslipped.

Enzyme histochemistry

In Papers I and II, enzyme histochemistry was used to determine the activities of cytochrome *c* oxidase (COX) and succinate dehydrogenase (SDH), to visualize mitochondrial function/dysfunction in tissue sections. The sequential COX/SDH double-labeling protocol used here is based on principles previously described (Seligman 1968; Old and Johnson 1989; Blanco et al. 1988; Dubowitz et al. 1973). COX, or complex IV, is a respiratory chain enzyme partially encoded by mtDNA, whereas SDH, or complex II, is entirely encoded by nDNA. Impaired expression of mtDNA typically leads to a pattern of marked reduction in complex IV activity, while complex II activity is preserved. Respiratory chain-deficient cells will stain blue with the COX/SDH double histochemistry method, whereas cells with normal respiratory chain function will appear dark brown.

Frozen 14-μm cryostat sections were air-dried for 1 h, and then incubated for 40 min at 37 °C with a mixture of 1X DAB (Sigma Liquid Substrate System D7304; Sigma), 100 μM cytochrome c, and 2 μg bovine catalase (2 μg ml^{-1} or approximately 4 IU mL^{-1}) in 0.1 M PBS (pH 7.0). The sections were then washed four times at 10 min in 0.1 M PBS (pH 7.0). Next, a mixture of 1.5 mM NBT, 1.3 M sodium succinate, 0.2 mM PMS, and 1.0 mM sodium azide in 0.1 M PBS (pH 7.0) was applied to the sections for 40 min at 37 °C. Sections were then washed (four times at 10 min in 0.1 M PBS, pH 7.0), dehydrated in increasing concentrations of ethanol (70%, 95%, and 99.5%), mounted (Entellan), coverslipped, and visualized under bright-field microscopy.

In Paper I, to determine any mitochondrial dysfunction indicated by blue staining, slides were coded, and key brain regions were semi-quantified for amount of blue stain on a blind basis using a scale of 0–4 (0, no blue staining; 4, only blue staining). Semi-quantification was performed bilaterally in cerebral cortex, hippocampus, nucleus accumbens, striatum, and thalamus, and mean values were calculated for each area and animal.

mRNA Expression

Oligonucleotide probes

In Papers I and III, DNA oligonucleotide probes were used for quantitative *in situ* hybridization (ISH) to detect levels of mRNA transcripts in defined brain regions and elsewhere. The accuracy of quantitative ISH has been verified by quantitative PCR (Broide et al. 2004). Synthetic oligonucleotide probes were ~50 bp long and had a guanine-cytosine (GC) content of 45%. Mfold web server software (version 3.2) was used to estimate the folding energy (Mathews et al. 1999; Zuker 2003). Probe specificity was confirmed by first aligning the probe against all publicly known sequences (www.ncbi.nlm.nih.gov/BLAST), and then cross-referencing the expression with published results from immunohistochemistry, in situ hybridization, and Northern blots.

Based on the above criteria, two oligonucleotide DNA probes (Thermo Scientific, Waltham, MA, USA) were designed and tested per gene, all of which worked, and one probe per gene was selected for mRNA quantization: LDH-A: 5′-CACAGGGGTAATCGAAGCCTGCAGTTGGCAGTGTGTCTCAGAGACAGT-3′; LDH-B: 5′-GCTTGATGACTTCATAGGCACTGTCCACCACCATCTTATGCACCTCCTTCC-3′; Nurr1: 5'-GCGTAGTGGCCACGTAGTTCTGGTGGAAGTTCTGAAGGGAGCCCGGATCG-3'. Additionally, a random probe with similar sequence length and GC content was used as a negative control, and consecutive sections from a wild-type littermate were inserted as a positive control in each experiment.

in situ Hybridization

High-stringency radioactive ISH was performed on tissue sections (brain, heart, and liver) based on the protocol established by Dagerlind et al. (Dagerlind et al. 1992) to determine mRNA levels. Probes were labeled with α-^{33}P-deoxyadenosine 5′-triphosphate (dATP) at the 3′ end (Perkin-Elmer, Boston, MA, USA) using terminal deoxynucleotidyl transferase (TdT) (Amersham Biosciences, Buckinghamshire, UK), and purified with ProbeQuant G50-Micro Columns (Amersham Biosciences). Cryosections were air-dried 3-5 h, and hybridized overnight at 42 °C in a humidified chamber with 150 µL of a mixture containing 4X SSC solution (3.0 M trisodium citrate and 3.0 M sodium chloride; pH 7.0), 50% formamide ($HCONH_2$), 1X Denhardt's solution (Ficoll, Polyvinylpyrrolidone, and BSA), 1% sarcosyl, 0.02 M sodium

phosphate (Na_3PO_4), 10% dextran sulfate (wt vol^{-1}), 0.2 M DTT ($C_4H_{10}O_2S_2$), 0.5 µg μL^{-1} sheared salmon serum sperm DNA, and the radio-labeled oligonucleotide. Slides were covered (Parafilm M; VWR International). The next day, slides were washed in 60 °C 1X SSC buffer five times for 1 h and cooled to RT, followed by rapid dehydration in increasing concentrations of ethanol (70%, 95%, and 99.5%), and finally, air-dried.

Image analysis

Visualization and quantification of mRNA content in sections were performed and expressed as nCi g^{-1}. Slides were exposed first to phosphoimaging plates (Fujix BAS-3000; Fuji Photo Film Co, Tokyo, Japan) for qualitative assurance and to determine appropriate film exposure time, and then to autoradiographic films (Biomax; Eastman Kodak Co, Rochester, NY, USA) together with ^{14}C standards (Amersham) from 2–5 days to 3-4 weeks, depending on the signal intensity of the radio-labeled oligonucleotide.

In Paper I, mRNA content was determined by digitizing the autoradiographic films (Epson Perfection V750 Pro; Epson, Nagano, Japan), and then quantifying the mRNA signal intensity (ImageJ, version 1.38, http://rsb.info.nih.gov/ij/). Optical density readings from scanned autoradiographs were converted to nCi g^{-1} as determined from a ^{14}C-step standard curve. Measurements of optical density from the autoradiographic films were made bilaterally in cerebral cortex and CA1 of hippocampus, and a mean value was calculated for each area and animal.

Microscopy

In Paper I – III, slides were examined and analyzed using either epifluorescence or bright-field microscopy (Zeiss Axiophot 2 microscope and Axioplan 2 Imaging Software; Carl Zeiss Light Microscopy, Göttingen, Germany). Images were processed using appropriate software (Adobe Photoshop CS5; Adobe Systems, San Jose, CA).

CHROMATOGRAPHIC-BASED TECHNIQUES

High-performance liquid chromatography

In Paper I, lactate levels were measured in tissue homogenates prepared with and without blood by high-performance liquid chromatography (HPLC).

Tissue preparation with blood

Animals were killed by cervical dislocation, and tissues including whole brain, liver, and heart were removed within 15–20 s, rapidly frozen in liquid nitrogen for 6 s, powdered over dry ice, and homogenized in 4 mL of 12% (vol vol^{-1}) perchloric acid ($HClO_4$) solution (wt vol^{-1}) at 0 °C using a polished glass tube pestle homogenizer. Blood was collected from the severed vessels and centrifuged 5 min at 4,000 x *g*, and 1 mL of 7% perchloric acid solution (vol vol^{-1}) was added to 1 mL plasma. Homogenates and plasma samples were centrifuged at 40,000 x *g* for 15 min, supernatants were placed in an ice bath, and neutralized to pH 4–5 with potassium hydroxide (KOH). Samples were centrifuged for another 15 min at 40,000 x *g* to sediment the precipitant potassium perchlorate ($KClO_4$), which formed after neutralization with KOH. Supernatants were retained and filtered (0.2 μm) before lyophilization.

Tissue preparation with blood removed

For tissue preparation with blood removed, animals were anesthetized with 40 mg kg^{-1} body weight pentobarbital (Taber and Irwin 1969), and arterial blood was collected and lyophilized as described above. Anesthetized animals were perfused with 20 mL Ca^{2+}-free Tyrode's solution, and whole brain, heart, and liver were rapidly removed, frozen, homogenized, and lyophilized as described above.

Determination of lactate

Lactate levels were determined by ion-exchange column liquid chromatography with UV detection. The HPLC system included a pump (BAS 460; Bioanalytical Systems, West Lafayette, IN, USA), a refrigerated microsampler (CMA-200; CMA/Microdialysis, Stockholm, Sweden), and a UV detector (BAS 116, operating at 214 nm; Bioanalytical Systems). Chromatograms were recorded and integrated by use

of a computerized data acquisition system (DataApex, Prague, Czech Republic). Lactate was separated on a 250 x 4.6 (internal diameter) mm Polypore H column (Bioanalytical Systems). The mobile phase consisted of 2.5 mM sulfuric acid (H_2SO_4) pumped at a flow rate of 0.3 mL min^{-1}. Lactate levels were expressed as mmol L^{-1} for plasma and μmol g^{-1} for tissue samples. This protocol is based on an effective procedure to measure lactate levels by Kehr (Kehr 1999).

ENZYMATIC CHARACTERIZATION TECHNIQUES

Tissue preparation

In Paper I, LDH isoenzymes and enzymatic activity were characterized in tissue samples. Animals were killed by cervical dislocation, the brains were quickly removed (within 15–20 s) and rinsed in 0.1 M PBS (pH 7.4), after which cerebral cortex was dissected within 5–10 s, rapidly frozen on dry ice, and stored in −80 °C. Tissue samples were homogenized in 100 mM PPB (pH 7.0) with 2 mM g^{-1} tissue of EDTA. Homogenates were centrifuged at 10,000 x *g* for 15 min at 4 °C, and the supernatants were collected for assays.

Measurement of protein concentration

Protein concentration was determined by a colorimetric reaction using a protein assay kit (#500–0111; Bio-Rad Laboratories, Hercules, CA, USA) according to the manufacturer's instructions. A tunable microplate reader (VersaMax; Molecular Devices, Sunnyvale, CA, USA) at 25 °C with absorbance at 750 nm was used, and concentrations were expressed as mg mL^{-1} determined by a BSA standard curve using appropriate software (SoftMax Pro; Molecular Devices).

Lactate dehydrogenase isoenzyme characterization

Native gel electrophoresis was used to separate and characterize the five known LDH isoenzymes in cerebral cortex using a published protocol (Acosta et al. 2005) based on

the procedure of Nissen and Schousboe (Nissen and Schousboe 1979). This assay allows for direct visualization of expressed LDH isoenzymes in their native state. This is not achievable using Western blot or immunohistochemistry. Samples (50-µg protein) were loaded into a 1.5% agarose gel in 25 mM Tris·HCl and 250 mM glycine (pH 9.5) buffer, with a 6X gel loading buffer consisting of 0.1% bromophenol blue, 15% glycerol, and 20 mM Tris·HCl (pH 8.0). Electrophoresis was conducted for 75 min at 150 V in a 5 mM Tris·HCl and 40 mM glycine (pH 9.5) running buffer. Gels were then washed briefly in 100 mM Tris·HCl (pH 8.5) buffer. To visualize LDH isoenzyme bands, the gel was incubated for 20 min at 37 °C in a solution containing lactate (3.24 mg mL^{-1}), NAD^+ (0.3 mg mL−1), NBT (0.8 mg mL−1), and PMS (0.167 mg mL−1) dissolved in 10 mM Tris·HCl (pH 8.5) buffer. LDH isoenzyme concentration was quantified (BioRad Quantity-One) and expressed as a percent isoform.

Lactate dehydrogenase activity

Spectrophotometric assays were used to determine LDH activity converting pyruvate (P) to lactate (L) as well as L to P in cerebral cortex, detected using a tunable microplate reader (VersaMax; Molecular Devices) and appropriate software (SoftMax Pro). For $LDH_{L\rightarrow P}$ activity determination, an LDH kit (#DLDH-100; BioAssay Systems, Hayward, CA, USA) was used according to the manufacturer's directions. LDH activity in tissue samples was detected at 25 °C with absorbance at 565 nm. For $LDH_{P\rightarrow L}$ activity determination, an assay was designed based on the procedure of Krieg et al. (Krieg et al. 1967). Tissue samples were diluted to 0.05 mg mL^{-1} in 500mM PPB (pH 7.5) and added to the LDH assay reagent containing 100 mM pyruvate and NADH (5 mg/20 mL of assay buffer) in 500 mM PPB at pH 7.5. The change in NADH absorbance was measured at 25 °C in 1-min intervals for 5 min at 340-nm absorbance. LDH activity data were calculated in IU mg^{-1} protein and were expressed as P:L ratio ($LDH_{P\rightarrow L}/LDH_{L\rightarrow P}$) and percent change in LDH activity.

STATISTICS

Data are presented to at least two significant digits as mean values (M), number of observations, percentages, percent changes, with SEM or SD. Statistical analyses were performed using a linear regression model, two-sided Fisher's exact test, Chi-square test, two-tailed unpaired t-test, one-way Kruskal–Wallis ANOVA, one-way ANOVA, and two-way between subjects ANOVA. Posthoc analyses were used in conjunction with ANOVA analyses. Statistics were performed with an α level of 0.05 using appropriate software (GraphPad Prizm, v.5.0c, GraphPad Software Inc, San Diego, CA). Significances are denoted in tables and figures with $*P < 0.05$, $**P < 0.01$, and $***P < 0.001$.

RESULTS AND DISCUSSION

This thesis attempts to address outstanding issues related to ageing *per se* and the consequences of somatic mtDNA mutations on the ageing process, particularly in the brain. It spans from techniques to monitor and possibly predict symptomatic stages of ageing using lactate ^{1}H-MRS (Paper I) to the investigation of possible dietary intervention as a treatment to counteract ageing (Paper IV). It explores the consequences of mtDNA mutation load during embryogenesis for brain development and ageing *per se* (Paper III), and also describes an important histochemical technique that can be used to visualize abnormal mitochondrial respiratory chain function in tissue sections (Paper II). While the focus of this work has been the mtDNA mutator mouse, the first experimental model to test the "Mitochondrial Theory of Aging", normally ageing wild-type mice were used when possible and similarities and differences with regard to the mtDNA mutator mouse were noted.

LACTATE AS A BIOMARKER OF THE AGEING PROCESS (PAPER I)

Currently, there are few means to track symptomatic stages of ageing, particularly in the brain. Such information could be useful for monitoring age-related alterations in neuronal function, and could also provide insights into age-related neurodegenerative diseases, such as Alzheimer's, Huntington's, and Parkinson's disease, as well as other forms of dementia and stroke. Metabolic changes have been implicated in the ageing process, but its direct linkage to mitochondrial dysfunction had not been established. Trifunovic *et al.* (Trifunovic et al. 2005) reported that MEFs from mtDNA mutator mice used less than 5% of the respiratory chain capacity of wild-type MEFs, which provided the first evidence that increasing somatic mtDNA mutations could lead to respiratory alterations in mtDNA mutator mice. However, the down-stream effects of progressively impaired oxidative phosphorylation and its effect on the ageing process in the brain remained unclear and largely unexplored.

Table 1. List of metabolites that can be detected and monitored *in vivo* using ^{1}H-magnetic resonance spectroscopy.

Metabolite	Abbreviation
γ-aminobutyric acid	GABA
creatine + phosphocreatine	Cr + PCr
glutamine and glutamate	Gln, Glu
lactate	Lac
myo-inositol	m-Ins
N-acetylaspartate	NAA
N-acetylaspartylglutamate	NAAG
taurine	Tau
macromolecules (M) and lipids (L)	ML-0.9, ML-1.4, ML-2.0, M-1.2, M-1.7

^{1}H-MRS was therefore used to detect any possible metabolic alterations occurring as a result of the somatic mtDNA mutations and impaired mitochondrial function. Proton-MRS was chosen over carbon- or phosphorous-MRS because it has a higher signal-to-noise ratio and provides a better sampling of a larger number of metabolites (Table 1). This non-invasive technique was used to monitor metabolic changes in two key brain areas, cerebral cortex and striatum, in mtDNA mutator mice and wild-type littermates from 6 – 42 weeks of age. Early in life and in advance of overt ageing phenotypes, the mtDNA mutator mice displayed a marked increase of the lactate doublet peak at 1.33 ppm in both brain areas (Fig 10). When lactate concentrations were estimated as ratios to total creatine concentrations, lactate levels were increased two-fold in both striatum and cerebral cortex as early as 6 weeks of age, and levels increased to three-fold in advanced age in cerebral cortex after 30 weeks of age. Interestingly, ^{1}H-MRS also detected an increase in lactate levels in wild-type mice after 20 weeks of age. HPLC was used to confirm the ^{1}H-MRS results, and to establish high brain lactate as a marker of normal ageing. Paper I describes the ^{1}H-MRS and HPLC results in full.

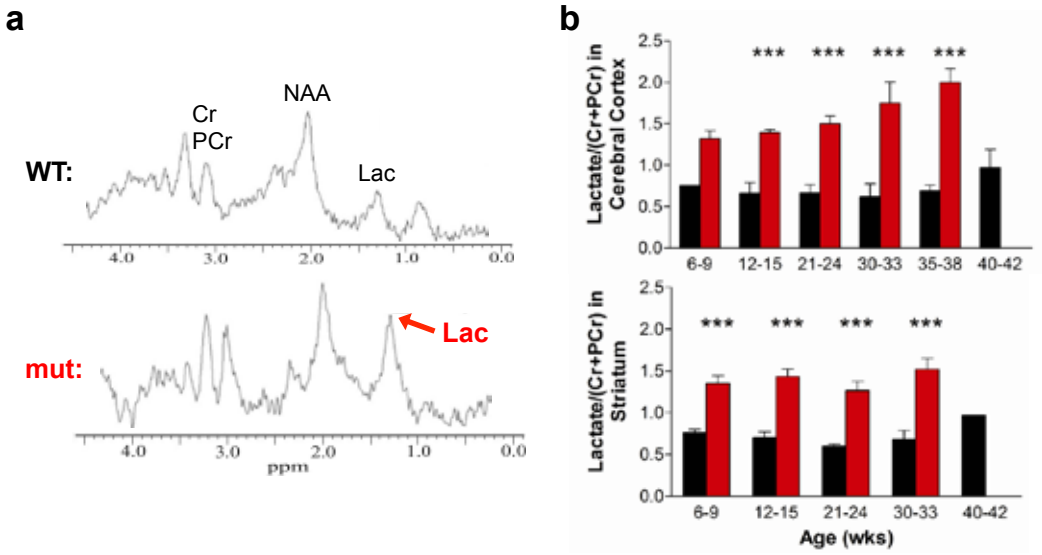

Figure 10. ^{1}H-MRS detected high lactate levels in brain. (a) Typical ^{1}H-MR spectra obtained from a VOI in cerebral cortex indicating the marked increase in the lactate doublet (centered on 1.33 ppm) in mtDNA mutator mice. (b) All mutator mice showed a significant increase in brain lactate concentrations, in cerebral cortex (upper) and striatum (lower) in female mtDNA mutator (red) compared with littermate wild-type (black) mice. *Modified from Ross* et al., PNAS, *2010 (Paper I).*

The findings in Paper I, coupled with other studies using MRS and biochemical assays to measure lactate and mitochondrial metabolism (Yesavage et al. 1982a; 1982b; Pryce et al. 1970; Boumezbeur et al. 2010; Zhang et al. 2009; Romanick 2004; Stacpoole 2012; Ertel et al. 2012; Kalpouzos et al. 2009; Yao et al. 2010; Bittles and Harper 1984; Goldstein et al. 1982), support a role for lactate as a marker in ageing, particularly in the brain. These data taken together, therefore, argue for the use of lactate ^{1}H-MRS as a noninvasive method to monitor this hallmark of the ageing process.

VISUALIZATION OF MITOCHONDRIAL RESPIRATORY FUNCTION (PAPER I AND II)

As described previously, mtDNA defects are an important cause of disease and may underlie ageing and ageing-related alterations (Larsson 2010; Cottrell et al. 2006). Observing the activity of respiratory enzymes is a straightforward approach for investigating mitochondrial dysfunction. Although other respiratory complexes could be investigated, complexes II and IV are the most amenable to histochemical examination (DiMauro and Hirano 2006; Old and Johnson 1989).

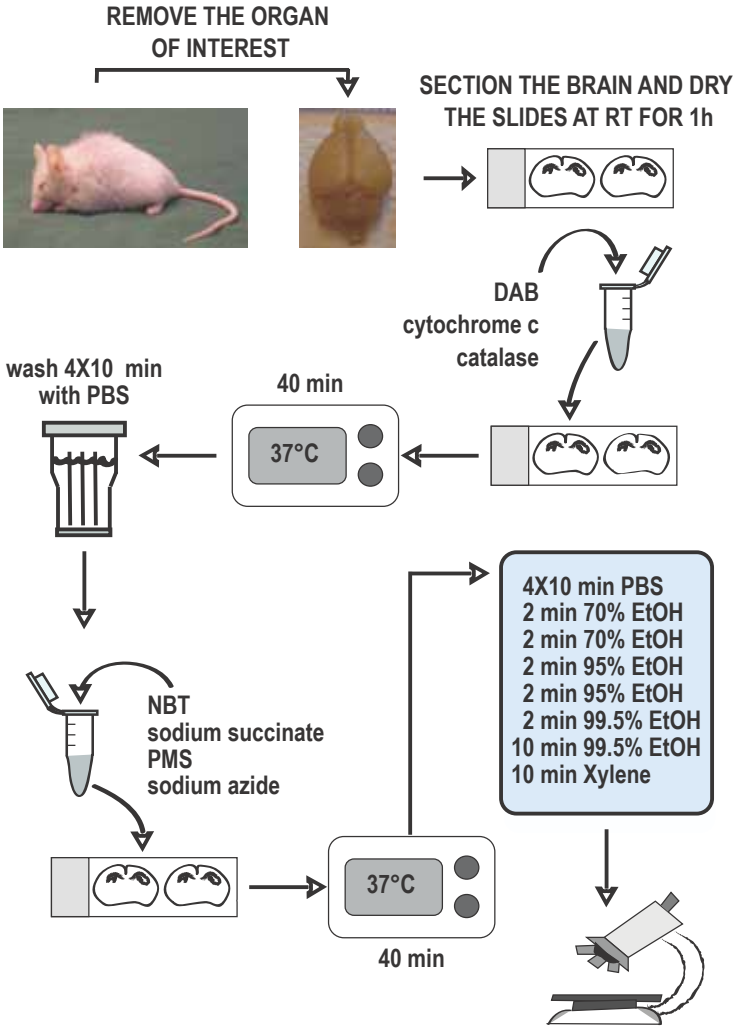

Figure 11. Flow chart of the COX/SDH double-labeling histochemical assay. Dissect the organs of interest and rapidly freeze the tissues. Collect cryostat sections and keep at -20°C until use. Air-dry sections at RT for 1 h. Incubate slides in medium for COX histochemistry for 40 min at 37°C. Wash the sections in PBS. Incubate the slides for SDH histochemistry for 40 min at 37°C. Wash the sections again in PBS, dehydrate in an ethanol series, mount, and coverslip the slides. *Modified from Ross,* JoVE, *2011, (Paper II).*

The catalytic subunits of complex IV, or COX, are encoded by mtDNA and are essential for assembly of the complex and mitochondrial function. Thus, proper synthesis and function are largely based on mtDNA integrity. In contract, complex II, or SDH, is entirely encoded by nDNA (see Figure 2 in Introduction), and its activity is typically not affected by impaired mtDNA. Hence, impaired mtDNA often leads to the presence of cells with low or absent COX activity (Cottrell et al. 2006; Seligman 1968; Dubowitz et al. 1973), and although the activities of COX and SDH can be investigated individually, the combined COX/SDH double-labeling method (Bonilla et al. 1992; DiMauro et al. 1990) has remained popular and has proven to be advantageous in

localizing cells with mitochondrial dysfunction (Brierley et al. 1998; Larsson et al. 1998; Ekstrand et al. 2007; Tulinius et al. 1991). In cells with functioning COX, the brown-colored DAB-product will localize in mitochondrial cristae and saturate cells. Cells with dysfunctional COX will therefore not be saturated by this DAB-product, allowing for the visualization of SDH activity and the formation of a blue-colored NBT-product. See Figure 11 for a flow chart of the COX/SDH double-labeling histochemical assay. Full experimental procedures are described in Paper II.

To correlate the striking increase in lactate (Paper I) with tissue histopathology, the sequential COX/SDH enzyme histochemical method was used to visualize reduced mitochondrial function in key brain regions of both prematurely ageing mtDNA mutator mice and normally ageing wild-type littermates. In mtDNA mutator mice, COX deficiencies (indicated by blue-color) began to decline at 9-12 weeks of age, and became widespread as the mice aged to 46 weeks (Fig 12). Decreased COX activity was also seen in similar brain regions of wild-type littermates as they aged to 130 weeks, indicating that altered mitochondrial function is a natural phenomenon of ageing, which is consistent with previous and recent reports (Cottrell et al. 2001; Kujoth et al. 2005; Brierley et al. 1998; Vermulst et al. 2008; Fox et al. 2012; Campbell et al. 2012; Horan et al. 2012).

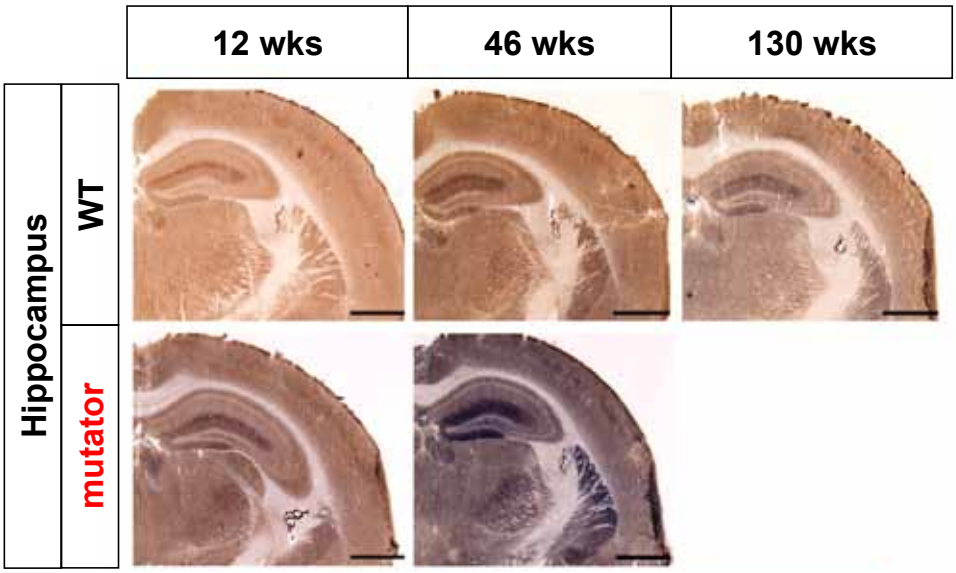

Figure 12. Mitochondrial dysfunction in ageing. COX/SDH double-labeling histochemistry was used to visualize respiratory chain deficiencies, indicated by blue staining, in brains of mtDNA mutator and wild-type mice. (Scale bar: 1.00 mm.) *Modified from Ross* et al., PNAS, *2010 (Paper I).*

ALTERATIONS IN LDH-A AND -B TRANSCRIPTIONAL ACTIVITIES (PAPER I)

The primary cause of the lactate pathology in mtDNA mutator mice is the progressive increase of mtDNA mutation frequency in mitochondria, which in turn causes dysfunction of the mitochondrial respiratory chain. One consequence of impaired mitochondrial function is impaired pyruvate oxidation, and increased pyruvate levels would be expected. Preliminary data indicate such an increase in pyruvate. Thus, cells would be forced to rely heavily on anaerobic metabolism to replenish NAD+, which is essential for glycolysis to continue, and its regeneration can be accomplished by converting pyruvate (P) to lactate (L) by lactate dehydrogenase (LDH; EC 1.1.1.27). This tetrameric enzyme arises from three genes, LDH-A, LDH-B and LDH-C (Li 1990). *Ldh-A* and *Ldh-B* products are expressed throughout the body including the CNS, whereas *Ldh-C* is exclusively found in testis (Gerhardt-Hansen 1968). LDH-A and LDH-B gene products, known as M and H respectively, combine to form five isoenzymes (Fig 13): LDH-1 (H_4), LDH-2 (H_3M_1), LDH-3 (H_2M_2), LDH-4 (H_1M_3) and LDH-5 (M_4), which differ in electrophoretic mobility, K_m lactate and K_m pyruvate (Miura 1966). LDH-1, for instance, has a K_m lactate of 1 mM, while LDH-5 has a K_m lactate of 5 mM (Buhl et al. 1977). Isoenzymes rich in H-subunits are inhibited by high concentrations of pyruvate, whereas isoenzymes dominated by M-subunits have optimal activity at such concentrations (Krieg et al. 1967). The tissue expression pattern of these five isoenzymes correlates with the relative proportion of anaerobic versus aerobic metabolism in different tissues (Markert et al. 1975).

Lactate Dehydrogenase Isoenzyme Composition

LDH-A gene Subunits (M)	*LDH-B* gene Subunits (H)	Isoenzyme
4	0	**LDH-5**
3	1	**LDH-4**
2	2	**LDH-3**
1	3	**LDH-2**
0	4	**LDH-1**

Figure 13. Lactate dehydrogenase (LDH) isoenzyme composition. LDH-A and LDH-B gene products (M and H) combine to form five tetrameric LDH isoenzymes.

In Paper I, experiments were designed to examine the LDH-A and –B gene expression and transcriptional activities, and the data revealed a shift in the LDH-A/B ratio to allow the tissue to counter the pyruvate increase, by promoting P to L conversion, which thus contributed to the increased lactate levels. Specifically, *in situ* hybridization was used to map and quantify transcriptional activity, and revealed an increase in LDH-A/-B gene expression ratio in cerebral cortex and CA1 of the hippocampus in both prematurely ageing mtDNA mutator mice and in wild-type littermates as they aged to 130 weeks (Fig 14). Altered LDH-A/-B gene expression was also present in cardiac muscle and hepatic tissue. Separation of LDH:1-5 in cerebral cortex from mtDNA mutator mice showed an increase in those enzymes chiefly comprised of the *Ldh-A* product (M subunit) and a decrease in the isoenzymes dominated by the *Ldh-B* product (H subunit), thus promoting P to L formation. LDH enzymatic activity was also measured in mtDNA mutator cerebral cortex from both the pyruvate and lactate sides of the reaction, and the data indicated a metabolic shift toward increasing lactate production. See Paper I for complete results. These results taken together indicate that the LDH-A and -B transcriptional activities are regulated allowing the formation of isoenzymes better suited to counteract impaired pyruvate oxidation (Ross et al. 2011). This has been supported by other recent studies (Bergersen and Gjedde 2012; Ben-Ari et al. 2011).

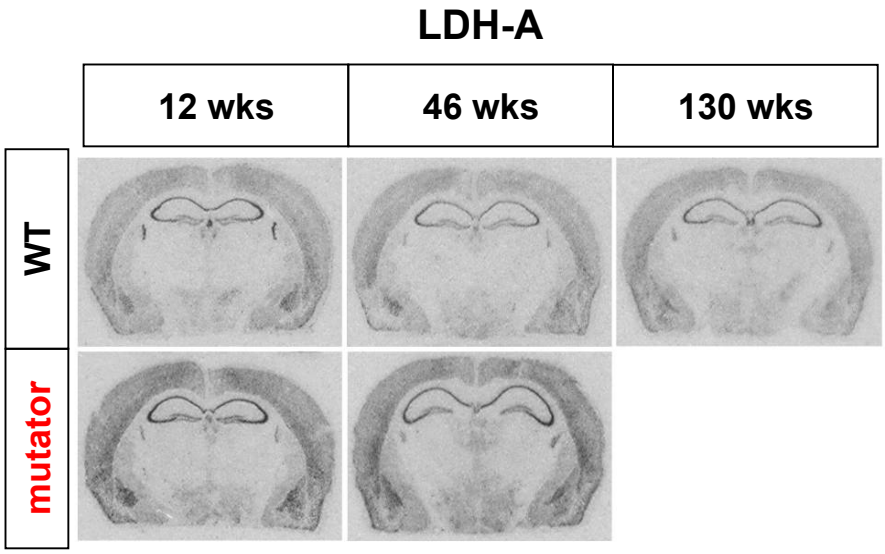

Figure 14. Lactate dehydrogenase expression in brain. *in situ* Hybridization was used to quantify mRNA levels of LDH-A (shown) and LDH-B (see Paper I) in prematurely ageing mtDNA mutator mice and normally ageing wild-type mice *Modified from Ross* et al., PNAS, *2010 (Paper I).*

POSSIBLE TREATMENTS TO COMBAT THE AGEING PROCESS (PAPER IV)

Identifying strategies to prevent and/or ameliorate ageing phenotypes in mtDNA mutator mice may provide valuable insights into the ageing process, and could lead to novel treatments for human age-related disease. Forced endurance exercise, commenced in early adulthood and practiced three times per week for five months, has been recently found to counteract progeroid ageing, decrease mtDNA mutation load, and increase mitochondrial biogenesis in similar prematurely ageing mtDNA mutator mice (Safdar et al. 2011). It was therefore hypothesized that dietary supplementation could also counteract premature ageing in mtDNA mutator mice. In Paper IV, a combined supplement called NT-020 plus BioVin® (NT-020-BV), which contains green tea, blueberry, and grape extract combined with carnosine, and vitamin D_3, was tested as a possible treatment strategy to ameliorate and/or combat premature ageing phenotypes in mtDNA mutator mice.

NT-020 was developed by screening more than 100 natural substances (Bickford et al. 2006), and has been found to promote stem cell proliferation, including human hematopoietic progenitors (Bickford et al. 2006) as well as adult neural stem cell proliferation after ischemic injury by middle cerebral artery occlusion (Yasuhara et al. 2008). Furthermore, NT-020 was found to improve learning and memory, and also to increase neurogenesis in aged rats after 4 weeks of treatment (Acosta et al. 2010).

Dietary treatment with NT-020-BV was begun in 20 week-old mtDNA mutator mice, when some visible progeroid symptoms were just starting. Age-matched wild-type littermates also received NT-020-BV *ad libitum*. See Paper IV for specific details regarding diet and housing. The condition of the animals was monitored weekly, and mice were tested 10 weeks after treatment began, and for some measurements also 20 weeks later. Significant improvement in spontaneous locomotor activity, determined by distance traveled and rearing, was found in 30 week-old mtDNA mutator mice after receiving NT-020-BV for 10 weeks (Fig 15). Gait performance was also assessed and normalization of mean paw intensity and significant amelioration in mean swing speed of both fore- and hind-limbs was found in 30 week-old mtDNA mutator mice after NT-020-BV diet supplementation. Moreover, marked improvements in motor programing was found in 30 and 40 week-old mtDNA mutator mice with treatment, determined by

the ability to learn and perform the locomotor task of crossing an elevated platform. Paper IV describes these results in detail.

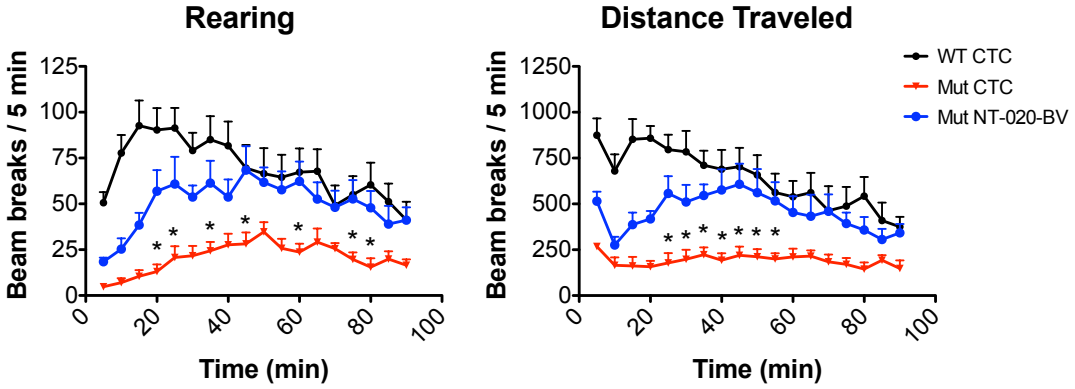

Figure 15. Spontaneous locomotion in mtDNA mutator mice. 30 week-old mtDNA mutator mice fed a control diet (Mut CTC) showed decreased rearing (left) and distance travelled (right) over a 90-minute period. However, 30 week-old mtDNA mutator mice treated with NT-020-BV for 10 weeks showed marked improvements in both parameters (Paper IV).

In addition to improved mobility and motor programming, the onset of other premature ageing phenotypes, including canities, alopecia, kyphosis, elongation of ears, and reduced body size, was delayed in mtDNA mutator mice fed a diet supplemented with NT-020-BV. Furthermore, an approximate 12% improvement of lifespan was found in mtDNA mutator mice receiving NT-020-BV (Fig 16). Symptoms such as enlargement of organs (heart, liver, spleen), sarcopenia, and loss of subcutaneous fat were also ameliorated. Lastly, mtDNA mutator mice receiving NT-020-BV showed increased nesting behavior (sign of improved cognition), cage cleanliness, grooming, and home-cage exploratory activity.

There are several studies suggesting that health- and life-span in humans can be influenced both negatively and positively by lifestyle choices, including exercise and diet (Rowe and Kahn 1987; Fiatarone et al. 1994; Hubert et al. 2002; Chernoff 2001). As previously mentioned, it was recently demonstrated that forced endurance exercise commenced in early adulthood has strikingly positive effects on prematurely ageing mice with the same proof-reading deficient PolgA mutation as the mtDNA mutator mice (Safdar et al. 2011). The findings of Paper IV indicate that the progeroid phenotype can also be improved by diet supplementation with natural substances, vitamins, and anti-oxidants (NT-020-BV) given from 20 weeks of age, at a time when

the mice are already developing some signs of premature ageing. Hence, starting diet intervention in early adulthood and/or combining exercise with diet intervention may have an even greater effect.

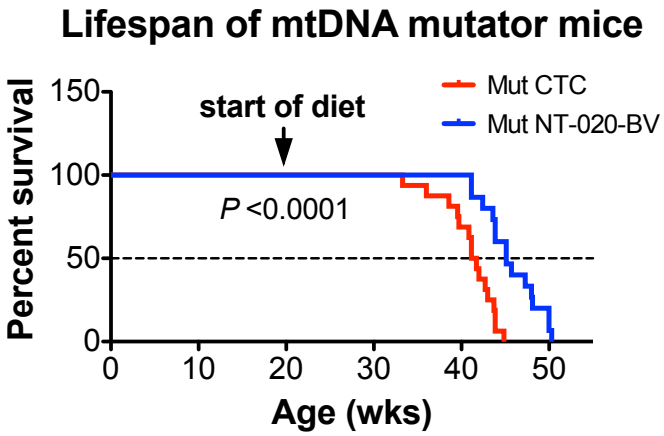

Figure 16. Longevity in mtDNA mutator mice. The mtDNA mutator mice fed a diet supplemented with NT-020 lived significantly longer than mtDNA mutator mice fed a control diet (Paper IV).

These diet data coupled with the results from exercise therapy by Safdar *et al.* (Safdar et al. 2011), support proof-of-principle that impaired mtDNA can influence ageing *per se*. The "Mitochondrial Theory of Aging" suggests that a key cause of ageing is progressive impairment of mtDNA and mitochondrial function; therefore, to support this hypothesis, animal models testing the theory should also be influenced by exercise and dietary interventions.

STOCHASTIC DISTURBANCES OF BRAIN DEVELOPMENT (PAPER III)

Increased mtDNA mutation load cause mtDNA mutator mice ($PolgA^{mut/mut}$) to develop a premature ageing syndrome. Somatic mtDNA mutations start to accumulate during embryogenesis and progressively increase throughout the lives of mtDNA mutator mice. Paper III describes the unexpected discovery that ~1/3 of the mtDNA mutator mice also exhibit stochastic, diverse brain malformations, ranging from major local perturbations of brain organization to symmetrical hippocampal and cortical migration disturbances, and suggests a possible mechanism for the formation of such brain disturbances.

Table 2. Brain disturbance demographics in mtDNA mutator mice (PolgA$^{mut/mut}$).

	No Disturbance		Visible Disturbance	*P*-value
PolgA$^{WT/WT}$	46 (100%)		0 (0%)	**<0.0001**
PolgA$^{mut/mut}$	28 (68%)		13 (32%)	
Female PolgA$^{mut/mut}$	10 (59%)		7 (41%)	0.322
Male PolgA$^{mut/mut}$	18 (75%)		6 (25%)	
	Focal Disturbance	***P*-value**	**Non-Focal Disturbance**	***P*-value**
PolgA$^{mut/mut}$	9 (69%)	**0.0004**	4 (31%)	**0.025**

Using cresyl violet or hematoxylin and eosin staining, visible brain malformations showing disturbed cell migration were documented in 41 mtDNA mutator mice (32%) from ages 7 to 46 weeks (Table 2). No brain disturbances were found in wild-type littermates or heterozygous mice. Disturbances that were widespread were categorized as "non-focal" (Fig 17), while those that were localized and typically asymmetric were termed "focal" (Fig 18). Although these brain disturbances typically did not correlate with overt behavioral manifestations, the nature of several of them suggests that they may have cognitive consequences.

"Non-focal" brain disturbances

Four mtDNA mutator brains were found to have "non-focal" disturbances; two of which were identical. Cortical lamination disturbances, primarily affecting layers III-IV in cerebral cortex, along with separation of stratum pyramidale in hippocampus into two layers were found in two 12 week-old female mtDNA mutator mice (Fig 17). ISH was used to locate the cells that express nuclear receptor related 1 (Nurr1), which are usually located in layers V-VI of cerebral cortex. In these two disturbed mtDNA mutator brains, the Nurr1 mRNA-expressing neurons were located in layers III-IV, suggesting that this particular type of disturbance is migratory, rather than due to altered proliferation. Additionally, two mice were found with hypertrophic/hyperplastic changes, presumably the result of increased proliferation or cell survival, with affected cerebral cortex, hippocampus, and cerebellum.

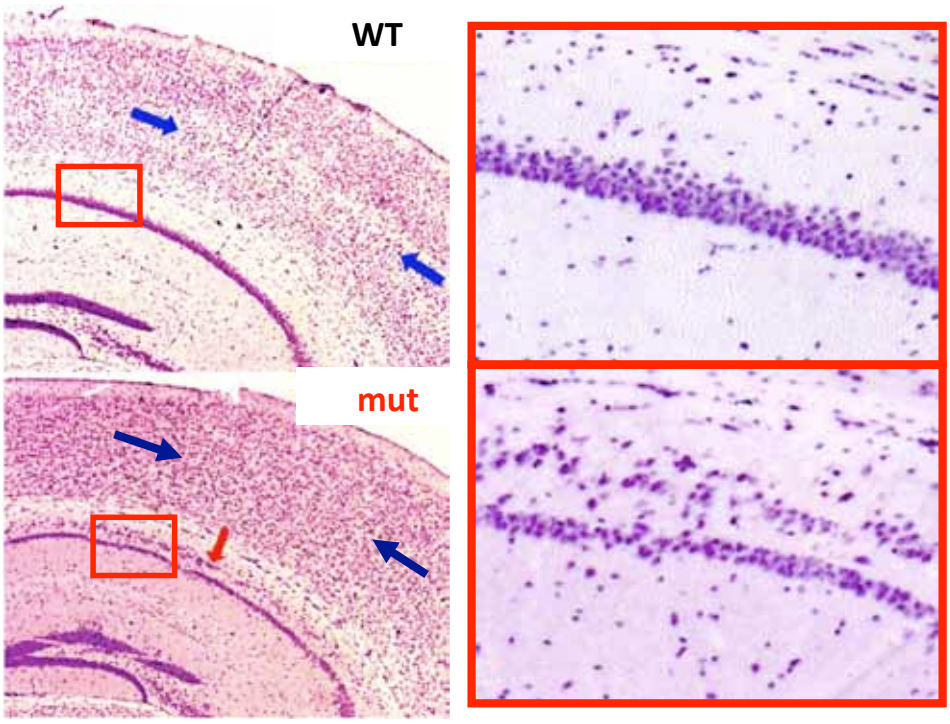

Figure 17. Non-focal brain disturbances in mtDNA mutator mice. Cresyl violet staining of hippocampal sections from 12 week-old mtDNA mutator and wild-type mice. Arrows indicate areas of cortical and hippocampal delamination (Paper III).

"Focal" brain disturbances

MRI detected an abnormal unilateral white matter signal in striatum and elongation of the right, anterior hippocampus in a 24 week-old male mtDNA mutator mouse. Subsequent histological study revealed striking mosaic subcortical perturbations and hippocampal malformations (Fig 18), and SDH enzyme histochemistry revealed areas of increased activity, presumably due to increased cell density or mitochondrial biogenesis. "Focal" brain disturbances were found in another eight mtDNA mutator mice, each with various malformations. They ranged from cerebellar malformations and brain stem asymmetry, to volumetric changes in thalamus causing asymmetry of hippocampus.

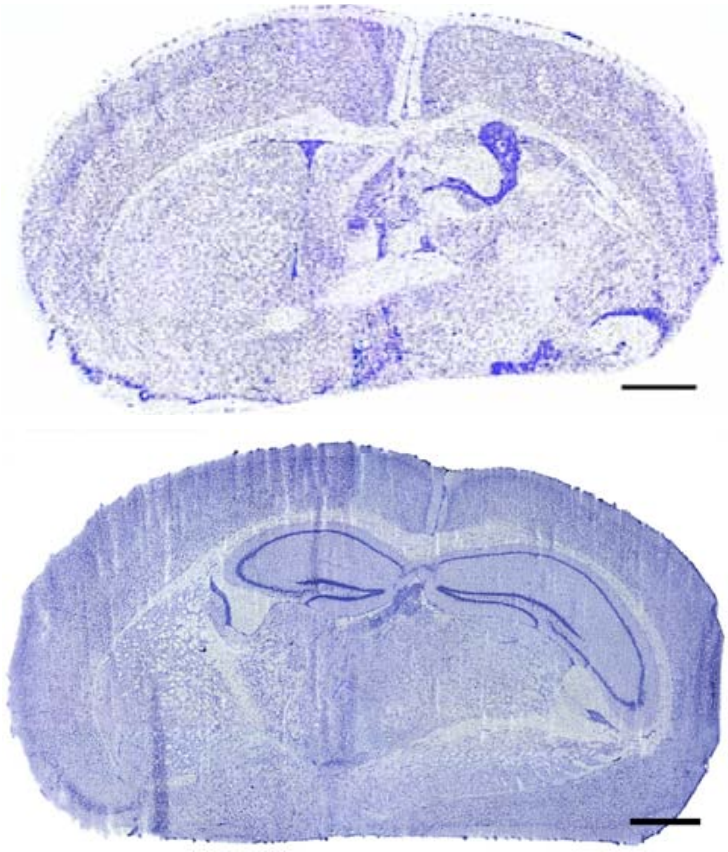

Figure 18. Focal brain disturbances in mtDNA mutator mice. Cresyl violet staining shows areas of severe cortical and sub-cortical malformations of striatum (upper) and anterior hippocampus (lower) in a 24 week-old mtDNA mutator mouse (Paper III).

POSSIBLE SOURCES OF MITOCHONDRIAL DNA MUTATION LOAD (PAPER III)

It was recently shown that there is maternal transmission of mtDNA mutations through the germ-line when intercrossing heterozygotes for several generations (Ameur et al. 2011). In mtDNA mutator mice there is thus the possibility to have both clonal expansion of maternally inherited mtDNA mutations, as well as the formation and expansion of *de novo* mutations. Hence, the formation of brain disturbances could be due to either one of these possibilities, or even both in combination. To further investigate this hypothesis, 3 lines of mtDNA mutator mice were created: (Line 1) intercrossing of heterozygotes ($PolgA^{mut/WT}$) for more than 10 generations; (Line 2) backcrossing of male heterozygotes with C57Bl/6 females for 4 generations to introduce wild-type mtDNA and nDNA; (Line 3) backcrossing of female heterozygotes with C57Bl/6 males for 4 generations to introduce wild-type nDNA only. See Figure 5 in Materials and Methods for this breeding schematic.

The mtDNA mutator mice from Lines 1 and 3 continued to show brain malformations, indicating that the re-introduction of healthy nDNA in Line 3 did not have an effect. Interestingly, no visible disturbances were found in Line 2 mtDNA mutator mice, suggesting that the insertion of healthy mtDNA had an effect on the presence of brain developmental malformations. Moreover, disturbances were not observed in wild-type or heterozygous mice from Lines 1 or 3, both with maternally inherited mtDNA mutations from intercrossing of heterozygotes. These data, coupled with the findings of Ameur *et al.* (Ameur et al. 2011), indicate that the brain disturbances are the result of a combination of maternally inherited mtDNA mutations and *de novo* mtDNA mutations during embryogenesis, both the result of dysfunctional PolgA. Paper III describes the characterization of the 3 lines of mtDNA mice in detail.

THE IMPORTANCE OF STARTING LIFE WITH HEALTHY MITOCHONDRIA (PAPER III)

In addition to the finding that an increase of maternally inherited mtDNA load increases the risk that offspring will develop brain disturbances, Paper III also describes clear effects on fecundity and fertility in the 3 different lines of mtDNA mutator mice. The degree to which mtDNA mutations present during embryogenesis impacts subsequent ageing is not well understood, particularly how ageing and age-related disorders progress in individuals who carry non-symptomatic disturbances in brain development. The different breeding schemes also provided valuable insights into the ageing process (Table 3). In addition to the improvements in fertility and viability of offspring in Line 2, lifespan was increased by more than 10% and the onset of progeroid ageing phenotypes including weight loss, graying, alopecia, kyphosis, and reduced body size was delayed. Thus, the extent of mtDNA mutation load during embryogenesis may also predict the rate of ageing *per se* in mtDNA mutator mice.

Somewhat akin to mtDNA mutator mice, individuals with Down syndrome also prematurely age, have reduced lifespan, and exhibit brain developmental malformations (Haydar and Reeves 2012; Lubec and Engidawork 2002). It has recently been shown that Down syndrome individuals also have anomalous neuronal gene expression during the critical period of synaptic maturation, which can alter neurogenesis, neuronal differentiation, myelination, and synaptogenesis (Kuhn et al. 2010). Mouse models of Down syndrome demonstrate key deficiencies in neural stem and progenitor cell

expansion and changes in the resulting specification of post-mitotic neurons and glial cells in the developing CNS (Haydar and Reeves 2012). Moreover, increased mtDNA mutations have been measured in both Down syndrome individuals as well as in their mothers (Busciglio et al. 2002; Del Bo et al. 2001; Arbuzova et al. 2001; 2002; Schon et al. 2000), and mitochondrial dysfunction has been reported in mouse models of Down syndrome (Bambrick and Fiskum 2008). Age-related increases in mtDNA mutations have been reported in oocytes (Keefe et al. 1995; Brenner et al. 1998; Schon et al. 2000) and the impairment of meiosis I and II (Strick et al. 2000), which can lead to aneuploidy. Lastly, it is noteworthy that impaired mtDNA and mitochondrial dysfunction are increasingly implicated in the etiology and pathogenesis of other neurological disorders, such as autism spectrum disorder, schizophrenia, bipolar disorder, and attention deficit disorder, all of which may be caused by disturbances of brain development (Caglayan 2010; Pettegrew et al. 1993; Weissman et al. 2008; Oliveira et al. 2005; Ichikawa et al. 2012; Verge et al. 2011; Marazziti et al. 2011).

Table 3. Description of the different lines of mtDNA mutator mice (genotype PolgA$^{mut/mut}$) obtained by intercross of heterozygous mice (genotype PolgA$^{mut/WT}$).

Line	Mother (PolgA$^{mut/WT}$)		mtDNA mutator mice (PolgA$^{mut/mut}$) phenotype
	Origin of mtDNA	**Origin of nuclear DNA**	
1	Intercrossed for many generations	Intercrossed for many generations	Typical mtDNA mutator ageing phenotype* Decreased fecundity ~ 30% brain malformations
2	Recent reintroduction of wild-type mtDNA	Recent reintroduction of wild-type nuclear DNA	Improved ageing phenotype Improved fecundity No visible brain malformations
3	Intercrossed for many generations	Recent reintroduction of wild-type nuclear DNA	No difference compared to Line 1

* As described by Trifunovic et al. 2004

The question arises as to the mechanism underlying the variety of focal and non-focal malformations and the fact that such malformations are not seen in all the mtDNA mutator mice. The clonal expansion of cells, in which defective transcription exists in the mtDNA mutator mice. Moreover, the nature of these disturbances suggests that they occur early in embryogenesis. These facts lead to the hypothesis that the malformations may be due to mitochondrial defects in stem cells leading to abnormal migration of neuronal and glial elements. This conjuncture is supported by a recent study by Ahlqvist *et al.* (Ahlqvist et al. 2012) with similar mice, showing that neural and hematopoietic progenitor cells had defects in self-renewal and differentiation from early in embryogenesis.

These studies coupled with our findings in Paper III, demonstrate a causative role for mtDNA mutations, both inherited and *de novo*, in the development of brain disturbances and neuropathological conditions. Moreover, these data provide evidence that the ageing process *per se* may be influenced by mtDNA mutation load during embryogenesis. Lastly, this work suggests that genetic abnormalities, which affect developmental disturbances of the brain, may be compensated in adulthood, but may contribute to dysfunction as the brain ages.

CONCLUSIONS

Paper I: Somatic mtDNA mutations can lead to metabolic disturbances

- A molecular link between progressive failure of oxidative phosphorylation and abnormal metabolism was established in the ageing process
- LDH-A and -B transcriptional activities are regulated to the formation of isoenzymes better suited to counteract impaired pyruvate oxidation in ageing
- Lactate ^{1}H-MRS can be used as a non-invasive strategy for monitoring, and possibly predicting the ageing process

Paper II: Visualization of mitochondrial function using enzyme histochemistry

- The activities of mitochondrial respiratory chain complexes (cytochrome *c* oxidase and succinate dehydrogenase) can be visualized with high reproducibility using a strict protocol for the double-labeling histochemical COX/SDH technique
- Somatic mtDNA mutations observed in mitochondrial diseases, ageing, and age-related diseases often leads to the presence of cells with low or absent respiratory chain function

Paper III: mtDNA Mutations can cause developmental disturbances in the brain

- Genetic variants that cause premature ageing can also cause stochastic developmental disturbances of the brain
- The same genetic mutation (PolgA) can cause many different types of developmental problems
- Occurrence of brain disturbances in mtDNA mutator mice is dependent on germline accumulation of mtDNA mutations in their heterozygous mothers
- The fact that mtDNA mutations can lead to stochastic developmental disturbances provides a novel mechanism for the variable pathology caused by mitochondrial dysfunction in mitochondrial disease and human malformations

Paper IV: Diet intervention can counteract premature ageing phenotypes

- Dietary supplementation with natural ingredients, vitamins, and anti-oxidants (NT-020-BV) delayed the onset of premature ageing phenotypes, ameliorated the overall health, and increased longevity in mtDNA mutator mice
- The "Mitochondrial Theory of Aging" suggests that a key cause of normal ageing is progressive impairment of mitochondrial function, caused by increased mtDNA mutations; and therefore, animal models testing this theory should be influenced by exercise and dietary interventions, since these lifestyle factors influence normal ageing in humans

CONCLUDING REMARKS

The overall goal of this thesis was to investigate how elevated somatic mtDNA mutations may translate to age-related functional changes in the central nervous system, using a transgenic mouse model of premature ageing, the mtDNA mutator mouse. The results of Paper I and II link the accumulation of mtDNA mutations with specific alterations in cellular respiration and the ageing process, giving rise to the use of lactate proton-magnetic resonance spectroscopy as a non-invasive method to track the ageing process. It is the hope that with additional research this technique could be applied to humans as a strategy to monitor symptomatic stages and possibly pre-symptomatic stages of brain ageing. Recent publications directly link changes in brain lactate production and its transport to mitochondrial dysfunction and neuronal loss, with similarities to patients with amyotrophic lateral sclerosis (Fünfschilling et al. 2012; Lee et al. 2012). Alterations in brain lactate might also be applicable to other age-related neurodegenerative diseases, such as Alzheimer's and Parkinson's disease.

Paper I also concludes that key enzymes of cellular respiration (LDH) can be regulated to counteract mitochondrial dysfunction. Although metabolic alterations are implicated in ageing, the manifestations remain unclear. Thus, it could be of interest to investigate LDH changes in the brains of normally ageing humans. Additional research could examine how the expression of LDH isoenzymes is regulated, and how the cell-specific distribution of these isoenzymes changes with age.

The results of Paper IV coupled with the findings of Safdar *et al.* (Safdar et al. 2011) indicate that lifestyle factors, such as diet and exercise, can have a major influence on the progression of ageing in the mtDNA mutator mice. The endurance exercise experiments described in Safdar *et al.* began in early adulthood (9-10 weeks of age), whereas the findings of Paper IV indicate that diet intervention, even when started in middle-aged (20 weeks old) mtDNA mutator mice, can markedly improve health and lifespan. Interestingly, a recent publication demonstrated a significant association between exercise commenced in middle-aged humans (average age 49 years) and a healthier outcome during 26 years of follow-up (Willis et al. 2012), suggesting that healthy lifestyle factors initiated even in midlife can markedly counteract morbidity.

What similarities, at a molecular level, are there between these lifestyle factors? Is it simply mitochondrial biogenesis? A recent publication by Dillon *et al.* indicates that increased mitochondrial biogenesis can ameliorate *some* of the premature ageing phenotypes in mtDNA mutator mice (Dillon et al. 2012); however, lifespan was not increased and the accumulation of mtDNA mutations was not decreased. Thus, additional experiments that are designed to isolate the possible mechanisms and the involvement of mitochondria are essential to understanding how to promote healthy ageing.

The discovery that at least 30% of mtDNA mutator mice have stochastic brain developmental disturbances in combination with results from the breeding schemes to reintroduce wild-type mtDNA have opened the door to re-evaluate the importance of starting life with healthy mitochondria. The findings of Paper III suggest that (i) an increase of maternally inherited mtDNA mutation load increases the risk that offspring will develop brain disturbances, (ii) maternally inherited mtDNA mutation load has clear effects on fecundity and fertility, (iii) the extent of mtDNA mutation load during embryogenesis may also predict the rate of ageing *per se*. How does the degree to which mtDNA mutations present during embryogenesis impact subsequent ageing? Particularly, how do ageing and age-related disorders progress in individuals who carry non-symptomatic disturbances of brain development? Although the results of Paper III provide a novel mechanism for the variable pathology caused by mitochondrial dysfunction in mitochondrial disease and with respect to human malformations, additional experimental research is needed to address these questions.

ACKNOWLEDGEMENTS

"Nani gigantum humeris insidentes", a Latin metaphor meaning "If I have seen further, it is by standing on the shoulders of giants", summarizes my feelings toward the amazing people that I have had the privilege to be surrounded by during this "PhD journey". It is because of my family, mentors, friends, colleagues, and collaborators that I have had the opportunity to do exciting science, and it will be because of your continued support and love that I will always push myself to do my very best, both in science and in life!

To my PhD supervisors and mentors, Barry and Lars. I cannot thank you enough for taking me under your wings. A mentor is supposed to be someone who sees the talent and ability within you, even more so than you may see, and helps to bring out those abilities to let them shine. You both have certainly done so, and it really has been a fantastic time. I feel honored to have been your student, and I can only hope to be the kind of mentor to my future students the way that you both have been to me.

To the National Institutes of Health – Karolinska Institutet Graduate Partnerships Program, thank you for having such an exceptional PhD program. Very important thanks to the National Institute on Drug Abuse, which has funded my PhD fellowship while in the partnerships program. I am also grateful to all the helpful and caring staff and directors at the NIH, NIDA, and KI. Special thanks to all the current and former NIH – KI GPP students, for forming a great support system to help navigate the unchartered waters of our unique PhD program.

To the current and past members of the Olson laboratory, thanks for the supportive environment and for helping to create a fun place to do science! As I continue on my scientific journey, I will bring with me such warm memories of my time in Stockholm. Through our interactions and discussions, you all have taught and inspired me to do good science and to "leave no stone unturned". A big thanks to the technical staff, Eva, Karin L, and Karin P, for sharing with me your "silent scientific knowledge" and for helping me when I needed it the most!

To my collaborators at the KI, NIH, NIDA, Max Planck, University of South Florida, University of Cologne, and University College London, who have contributed to many scientific aspects in this thesis. Thanks for your creative additions, ideas, and support. Together we have pursued some exciting scientific questions!

To current and former colleagues at the KI, thanks for creating a dynamic environment where cutting-edge science and jaw-aching fun often mixed! Thank you for *fika* in the winter and *glasspaus* in the summer. Special thanks to my colleagues in the animal facility at Retzius for all your help and support. It has been an honor to work alongside you all during my years in Stockholm.

To all my friends that I have made during my time in Stockholm and in Bethesda, and to those friends I made long, long before my PhD journey even began. You ALL have a very special place in my heart. You were always available to help celebrate all achievements, both small and large, or to bury any woes. I deeply cherish all of these friendships, and I look forward to sharing future experiences for years to come as our journeys continue to unfold!

To my family, and in particular my parents, this thesis is dedicated to you all. At the end of the day, when I am spent, I think of you. In the morning, when I am wearied, I think of you. You give me the strength to continue, to try my best, to work harder, and to never be complacent. You are so much a part of me; you are my North Star, and the small clear voices in my heart that will be with me always.

To my husband, Giuseppe – I saved the best for last! Thank you for coming on this "Swedish adventure" with me, and for being my partner-in-crime, both at home and in the lab. Over the past five years, our marriage has gone from a flower in bloom to a tender young fruit, and I very much look forward to many more years with you to watch this fruit mature. *Lovo solo a ti!*

REFERENCES

Ackl N, Ising M, Schreiber YA, Atiya M, Sonntag A, Auer DP. 2005. Hippocampal metabolic abnormalities in mild cognitive impairment and Alzheimer's disease. *Neurosci Lett* **384**: 23–28.

Acosta ML, Fletcher EL, Azizoglu S, Foster LE, Farber DB, Kalloniatis M. 2005. Early markers of retinal degeneration in rd/rd mice. *Mol Vis* **11**: 717–728.

Acosta S, Jernberg J, Sanberg CD, Sanberg PR, Small BJ, Gemma C, Bickford PC. 2010. NT-020, a natural therapeutic approach to optimize spatial memory performance and increase neural progenitor cell proliferation and decrease inflammation in the aged rat. *Rejuvenation Res* **13**: 581–588.

Ahlqvist KJ, Hämäläinen RH, Yatsuga S, Uutela M, Terzioglu M, Götz A, Forsström S, Salven P, Angers-Loustau A, Kopra OH, et al. 2012. Somatic progenitor cell vulnerability to mitochondrial DNA mutagenesis underlies progeroid phenotypes in Polg mutator mice. *Cell Metabolism* **15**: 100–109.

Alberts B. 2008. *Molecular biology of the cell*. Garland Pub.

Ameur A, Stewart JB, Freyer C, Hagström E, Ingman M, Larsson N-G, Gyllensten U. 2011. Ultra-Deep Sequencing of Mouse Mitochondrial DNA: Mutational Patterns and Their Origins. *PLoS Genet* **7**: e1002028.

Anderson AS, Loeser RF. 2010. Why is osteoarthritis an age-related disease? *Best Pract Res Clin Rheumatol* **24**: 15–26.

Anderson S, Bankier AT, Barrell BG, de Bruijn MH, Coulson AR, Drouin J, Eperon IC, Nierlich DP, Roe BA, Sanger F, et al. 1981. Sequence and organization of the human mitochondrial genome. *Nature* **290**: 457–465.

Arbuzova S, Cuckle H, Mueller R, Sehmi I. 2001. Familial Down syndrome: evidence supporting cytoplasmic inheritance. *Clin Genet* **60**: 456–462.

Arbuzova S, Hutchin T, Cuckle H. 2002. Mitochondrial dysfunction and Down's syndrome. *Bioessays* **24**: 681–684.

Bambrick LL, Fiskum G. 2008. Mitochondrial dysfunction in mouse trisomy 16 brain. *Brain Res* **1188**: 9–16.

Ben-Ari Y, Tyzio R, Nehlig A. 2011. Excitatory action of GABA on immature neurons is not due to absence of ketone bodies metabolites or other energy substrates. *Epilepsia* **52**: 1544–1558.

Bender A, Krishnan KJ, Morris CM, Taylor GA, Reeve AK, Perry RH, Jaros E, Hersheson JS, Betts J, Klopstock T, et al. 2006. High levels of mitochondrial DNA deletions in substantia nigra neurons in aging and Parkinson disease. *Nat Genet* **38**: 515–517.

Bergersen LH, Gjedde A. 2012. Is lactate a volume transmitter of metabolic states of the brain? *Front Neuroenergetics* **4**: 5.

Bernad A, Blanco L, Lázaro JM, Martín G, Salas M. 1989. A conserved 3"----5" exonuclease active site in prokaryotic and eukaryotic DNA polymerases. *Cell* **59**: 219–228.

Bickford PC, Tan J, Shytle RD, Sanberg CD, El-Badri N, Sanberg PR. 2006. Nutraceuticals Synergistically Promote Proliferation of Human Stem Cells. *Stem Cells and Development* **15**: 118–123.

Birky CW. 2001. The inheritance of genes in mitochondria and chloroplasts: laws, mechanisms, and models. *Annu Rev Genet* **35**: 125–148.

Bittles AH, Harper N. 1984. Increased glycolysis in ageing cultured human diploid fibroblasts. *Biosci Rep* **4**: 751–756.

Blanco CE, Sieck GC, Edgerton VR. 1988. Quantitative histochemical determination of succinic dehydrogenase activity in skeletal muscle fibres. *Histochem J* **20**: 230–243.

Bogenhagen D, Clayton DA. 1977. Mouse L cell mitochondrial DNA molecules are selected randomly for replication throughout the cell cycle. *Cell* **11**: 719–727.

Bogenhagen DF. 2012. Mitochondrial DNA nucleoid structure. *Biochim Biophys Acta* **1819**: 914–920.

Bonilla E, Sciacco M, Tanji K, Sparaco M, Petruzzella V, Moraes CT. 1992. New morphological approaches to the study of mitochondrial encephalomyopathies. *Brain Pathol* **2**: 113–119.

Boumezbeur F, Mason GF, de Graaf RA, Behar KL, Cline GW, Shulman GI, Rothman DL, Petersen KF. 2010. Altered brain mitochondrial metabolism in healthy aging as assessed by in vivo magnetic resonance spectroscopy. *J Cereb Blood Flow Metab* **30**: 211–221.

Brenner C, Wolny Y, Barritt J, Matt D, Munne S, Cohen J. 1998. Mitochondrial DNA deletion in human oocytes and embryos. *Mol Hum Reprod* **4**: 887–892.

Brierley EJ, Johnson MA, Lightowlers RN, James OFW, Turnbull DM. 1998. Role of mitochondrial DNA mutations in human aging: Implications for the central nervous system and muscle. *Ann Neurol* **43**: 217–223.

Broide R, Trembleau A, Ellison J, Cooper J, Lo D, Young W, Morrison J, Bloom F. 2004. Standardized quantitative in situ hybridization using radioactive oligonucleotide probes for detecting relative levels of mRNA transcripts verified by real-time PCR. *Brain Res* **1000**: 211–222.

Brown DT, Samuels DC, Michael EM, Turnbull DM, Chinnery PF. 2001. Random genetic drift determines the level of mutant mtDNA in human primary oocytes. *Am J Hum Genet* **68**: 533–536.

Brown WM, George M, Wilson AC. 1979. Rapid evolution of animal mitochondrial DNA. *Proc Natl Acad Sci USA* **76**: 1967–1971.

Buhl SN, Jackson KY, Vanderlinde RE. 1977. The effect of temperature on the kinetic constants of human lactate dehydrogenase 1 and 5. *Clin Chim Acta* **80**: 265–270.

Busciglio J, Pelsman A, Wong C, Pigino G, Yuan M, Mori H, Yankner BA. 2002. Altered metabolism of the amyloid beta precursor protein is associated with mitochondrial dysfunction in Down's syndrome. *Neuron* **33**: 677–688.

Caglayan AO. 2010. Genetic causes of syndromic and non-syndromic autism. *Dev Med Child Neurol* **52**: 130–138.

Campbell GR, Kraytsberg Y, Krishnan KJ, Ohno N, Ziabreva I, Reeve A, Trapp BD, Newcombe J, Reynolds R, Lassmann H, et al. 2012. Clonally expanded mitochondrial DNA deletions within the choroid plexus in multiple sclerosis. *Acta Neuropathol* **124**: 209–220.

Carrel A, Ebeling AH. 1921. Age and Multiplication of Fibroblasts. *J Exp Med* **34**: 599–623.

Castro-Gago M, Blanco-Barca MO, Campos-González Y, Arenas-Barbero J, Pintos-Martínez E, Eirís-Puñal J. 2006. Epidemiology of pediatric mitochondrial respiratory chain disorders in northwest Spain. *Pediatr Neurol* **34**: 204–211.

Chan DC. 2006. Mitochondria: Dynamic Organelles in Disease, Aging, and Development. *Cell* **125**: 1241–1252.

Chernoff R. 2001. Nutrition and Health Promotion in Older Adults. *J Gerontol A Biol Sci Med Sci* **56**: 47–53.

Chinnery P, Turnbull D. 2001. Epidemiology and treatment of mitochondrial disorders. *Am J Med Genet* **106**: 94–101.

Chinnery PF, Johnson MA, Wardell TM, Singh-Kler R, Hayes C, Brown DT, Taylor RW, Bindoff LA, Turnbull DM. 2000. The epidemiology of pathogenic mitochondrial DNA mutations. *Ann Neurol* **48**: 188–193.

Christensen K, Doblhammer G, Rau R, Vaupel JW. 2009. Ageing populations: the challenges ahead. *Lancet* **374**: 1196–1208.

Chuang C-S, Su H-L, Cheng F-C, Hsu S-H, Chuang C-F, Liu C-S. 2010. Quantitative evaluation of motor function before and after engraftment of dopaminergic neurons in a rat model of Parkinson's disease. *J Biomed Sci* **17**: 9.

Collado M, Blasco MA, Serrano M. 2007. Cellular senescence in cancer and aging. *Cell* **130**: 223–233.

Collado M, Serrano M. 2010. Senescence in tumours: evidence from mice and humans. *Nat Rev Cancer* **10**: 51–57.

Corral-Debrinski M, Horton T, Lott MT, Shoffner JM, Flint Beal M, Wallace DC. 1992. Mitochondrial DNA deletions in human brain: regional variability and increase with advanced age. *Nat Genet* **2**: 324–329.

Cortopassi GA, Arnheim N. 1990. Detection of a specific mitochondrial DNA deletion in tissues of older humans. *Nucleic Acids Res* **18**: 6927–6933.

Cottrell D, Turnbull D. 2000. Mitochondria and ageing. *Curr Opin Clin Nutr Metab Care* **3**: 473–478.

Cottrell DA, Blakely EL, Borthwick GM, Johnson MA, TAYLOR GA, BRIERLEY EJ, Ince PG, Turnbull DM. 2006. Role of Mitochondrial DNA Mutations in Disease and Aging. *Annals of the New York Academy of Sciences* **908**: 199–207.

Cottrell DA, Blakely EL, Johnson MA, Ince PG, Borthwick GM, Turnbull DM. 2001. Cytochrome c oxidase deficient cells accumulate in the hippocampus and choroid plexus with age. *Neurobiol Aging* **22**: 265–272.

Cottrell DA, Borthwick GM, Johnson MA, Ince PG, Turnbull DM. 2002. The role of cytochrome c oxidase deficient hippocampal neurones in Alzheimer's disease. *Neuropathol Appl Neurobiol* **28**: 390–396.

Dagerlind A, Friberg K, Bean AJ, Hökfelt T. 1992. Sensitive mRNA detection using unfixed tissue: combined radioactive and non-radioactive in situ hybridization histochemistry. *Histochemistry* **98**: 39–49.

Del Bo R, Comi GP, Perini MP, Strazzer S, Bresolin N, Scarlato G. 2001. Down's syndrome fibroblasts anticipate the accumulation of specific ageing-related mtDNA mutations. *Ann Neurol* **49**: 137–138.

Detmer SA, Chan DC. 2007. Functions and dysfunctions of mitochondrial dynamics. *Nat Rev Mol Cell Biol* **8**: 870–879.

Dillon LM, Williams SL, Hida A, Peacock JD, Prolla TA, Lincoln J, Moraes CT. 2012. Increased mitochondrial biogenesis in muscle improves aging phenotypes in the mtDNA mutator mouse. *Hum Mol Genet* **21**: 2288–2297.

DiMauro S, Bonilla E, Lombes A, Shanske S, Minetti C, Moraes CT. 1990. Mitochondrial encephalomyopathies. *Neurol Clin* **8**: 483–506.

DiMauro S, Hirano M. 2006. Approaches to the treatment of mitochondrial diseases. *Muscle & nerve*.

Dröge W. 2002. Free radicals in the physiological control of cell function. *Physiol Rev* **82**: 47–95.

Dubowitz V, Brooke MH, Neville HE. 1973. *Muscle biopsy*. W.B. Saunders Company.

Edgar D, Shabalina I, Camara Y, Wredenberg A, Calvaruso MA, Nijtmans L, Nedergaard J, Cannon B, Larsson N-G, Trifunovic A. 2009. Random point mutations with major effects on protein-coding genes are the driving force behind premature aging in mtDNA mutator mice. *Cell Metabolism* **10**: 131–138.

Ekstrand MI, Terzioglu M, Galter D, Zhu S, Hofstetter C, Lindqvist E, Thams S, Bergstrand A, Hansson FS, Trifunovic A, et al. 2007. Progressive parkinsonism in mice with respiratory-chain-deficient dopamine neurons. *Proc Natl Acad Sci USA* **104**: 1325–1330.

Ernster L, Schatz G. 1981. Mitochondria: a historical review. *J Cell Biol* **91**: 227s–255s.

Ertel A, Tsirigos A, Whitaker-Menezes D, Birbe RC, Pavlides S, Martinez-Outschoorn UE, Pestell RG, Howell A, Sotgia F, Lisanti MP. 2012. Is cancer a metabolic rebellion against host aging? In the quest for immortality, tumor cells try to save themselves by boosting mitochondrial metabolism. *Cell cycle* **11**: 253–263.

Fayet G, Jansson M, Sternberg D, Moslemi A-R, Blondy P, Lombès A, Fardeau M, Oldfors A. 2002. Ageing muscle: clonal expansions of mitochondrial DNA point mutations and deletions cause focal impairment of mitochondrial function. *Neuromuscul Disord* **12**: 484–493.

Fiatarone M, O'Neill E, Ryan N. 1994. Exercise Training and Nutritional Supplementation for Physical Frailty in Very Elderly People. *The New England journal of medicine* **330**: 1669–1775.

Flores I, Cayuela ML, Blasco MA. 2005. Effects of telomerase and telomere length on epidermal stem cell behavior. *Science* **309**: 1253–1256.

Fox RG, Magness S, Kujoth GC, Prolla TA, Maeda N. 2012. Mitochondrial DNA polymerase editing mutation, PolgD257A, disturbs stem-progenitor cell cycling in the small intestine and restricts excess fat absorption. *Am J Physiol Gastrointest Liver Physiol* **302**: G914–24.

Frederick BD, Lyoo IK, Satlin A, Ahn KH, Kim MJ, Yurgelun-Todd DA, Cohen BM, Renshaw PF. 2004. In vivo proton magnetic resonance spectroscopy of the temporal lobe in Alzheimer's disease. *Prog Neuropsychopharmacol Biol Psychiatry* **28**: 1313–1322.

Frenzel H, Feimann J. 1984. Age-dependent structural changes in the myocardium of rats. A quantitative light- and electron-microscopic study on the right and left chamber wall. *Mech Ageing Dev* **27**: 29–41.

Fünfschilling U, Supplie LM, Mahad D, Boretius S, Saab AS, Edgar J, Brinkmann BG, Kassmann CM, Tzvetanova ID, Möbius W, et al. 2012. Glycolytic oligodendrocytes maintain myelin and long-term axonal integrity. *Nature* **485**: 517–521.

Gann PH, Hennekens CH, Ma J, Longcope C, Stampfer MJ. 1996. Prospective study of sex hormone levels and risk of prostate cancer. *J Natl Cancer Inst* **88**: 1118–1126.

Gerhardt-Hansen W. 1968. Lactate dehydrogenase isoenzymes in the central nervous system : theoretical aspects and practical application in the diagnosis of brain tumors. *Danish Medical Bullentin* **S 15**: 1–112.

Giles RE, Blanc H, Cann HM, Wallace DC. 1980. Maternal inheritance of human mitochondrial DNA. *Proc Natl Acad Sci USA* **77**: 6715–6719.

Goldstein S, Ballantyne SR, Robson AL, Moerman EJ. 1982. Energy metabolism in cultured human fibroblasts during aging in vitro. *J Cell Physiol* **112**: 419–424.

Graziewicz MA, Longley MJ, Copeland WC. 2006. DNA polymerase gamma in mitochondrial DNA replication and repair. *Chem Rev* **106**: 383–405.

Guarente L. 2008. *Molecular Biology of Aging*. Cold Spring Harbor Laboratory Press.

Guarente L, Kenyon C. 2000. Genetic pathways that regulate ageing in model organisms. *Nature* **408**: 255–262.

Haas RH, Parikh S, Falk MJ, Saneto RP, Wolf NI, Darin N, Cohen BH. 2007. Mitochondrial disease: a practical approach for primary care physicians. *Pediatrics* **120**: 1326–1333.

Hamers FPT, Koopmans GC, Joosten EAJ. 2006. CatWalk-assisted gait analysis in the assessment of spinal cord injury. *J Neurotrauma* **23**: 537–548.

Harman D. 1956. Aging: a theory based on free radical and radiation chemistry. *J Gerontol* **11**: 298–300.

Harman D. 1972. The biologic clock: the mitochondria? *J Am Geriatr Soc* **20**: 145–147.

Haydar TF, Reeves RH. 2012. Trisomy 21 and early brain development. *Trends Neurosci* **35**: 81–91.

Hayflick L, Moorhead PS. 1961. The serial cultivation of human diploid cell strains. *Exp Cell Res* **25**: 585–621.

Herbener GH. 1976. A morphometric study of age-dependent changes in mitochondrial population of mouse liver and heart. *J Gerontol* **31**: 8–12.

Horan MP, Pichaud N, Ballard JWO. 2012. Review: Quantifying Mitochondrial Dysfunction in Complex Diseases of Aging. *J Gerontol A Biol Sci Med Sci*.

Howell N. 1997. Leber hereditary optic neuropathy: mitochondrial mutations and degeneration of the optic nerve. *Vision Res* **37**: 3495–3507.

Hubert HB, Bloch DA, Oehlert JW, Fries JF. 2002. Lifestyle habits and compression of morbidity. *J Gerontol A Biol Sci Med Sci* **57**: M347–51.

Hudson G, Chinnery PF. 2006. Mitochondrial DNA polymerase-gamma and human disease. *Hum Mol Genet* **15 Spec No 2**: R244–52.

Ichikawa T, Arai M, Miyashita M, Arai M, Obata N, Nohara I, Oshima K, Niizato K, Okazaki Y, Doi N, et al. 2012. Schizophrenia: maternal inheritance and heteroplasmy of mtDNA mutations. *Mol Genet Metab* **105**: 103–109.

James AM, Collins Y, Logan A, Murphy MP. 2012. Mitochondrial oxidative stress and the metabolic syndrome. *Trends Endocrinol Metab* **23**: 429–434.

Kaguni LS. 2004. DNA polymerase gamma, the mitochondrial replicase. *Annu Rev Biochem* **73**: 293–320.

Kalpouzos G, Chételat G, Baron J-C, Landeau B, Mevel K, Godeau C, Barré L, Constans J-M, Viader F, Eustache F, et al. 2009. Voxel-based mapping of brain gray matter volume and glucose metabolism profiles in normal aging. *Neurobiol Aging* **30**: 112–124.

Keefe DL, Niven-Fairchild T, Powell S, Buradagunta S. 1995. Mitochondrial deoxyribonucleic acid deletions in oocytes and reproductive aging in women. *Fertil Steril* **64**: 577–583.

Kehr J. 1999. *Modern Techniques in Neuroscience Research (Springer Lab Manuals)*. 1st ed. eds. U. Windhorst and H. Johansson. Springer.

Kenyon CJ. 2010. The genetics of ageing. *Nature* **464**: 504–512.

Khaidakov M, Heflich RH, Manjanatha MG, Myers MB, Aidoo A. 2003. Accumulation of point mutations in mitochondrial DNA of aging mice. *Mutat Res* **526**: 1–7.

Kirkwood TB. 1977. Evolution of ageing. *Nature* **270**: 301–304.

Kirkwood TB, Austad SN. 2000. Why do we age? *Nature* **408**: 233–238.

Kirkwood TBL. 2010. Global aging and the brain. *Nutr Rev* **68 Suppl 2**: S65–9.

Kirkwood TBL. 2005a. Time of our lives. What controls the length of life? *EMBO Rep* **6 Spec No**: S4–8.

Kirkwood TBL. 2005b. Understanding the odd science of aging. *Cell* **120**: 437–447.

Klass MR. 1983. A method for the isolation of longevity mutants in the nematode Caenorhabditis elegans and initial results. *Mech Ageing Dev* **22**: 279–286.

Kopecky B, Decook R, Fritzsch B. 2012. Mutational ataxia resulting from abnormal vestibular acquisition and processing is partially compensated for. *Behav Neurosci* **126**: 301–313.

Korhonen JA, Pham XH, Pellegrini M, Falkenberg M. 2004. Reconstitution of a minimal mtDNA replisome in vitro. *EMBO J* **23**: 2423–2429.

Kraytsberg Y, Kudryavtseva E, McKee AC, Geula C, Kowall NW, Khrapko K. 2006. Mitochondrial DNA deletions are abundant and cause functional impairment in aged human substantia nigra neurons. *Nat Genet* **38**: 518–520.

Krieg AF, Rosenblum LJ, Henry JB. 1967. Lactate dehydrogenase isoenzymes a comparison of pyruvate-to-lactate and lactate-to-pyruvate assays. *Clinical Chemistry* **13**: 196–203.

Kuhn DE, Nuovo GJ, Terry AV, Martin MM, Malana GE, Sansom SE, Pleister AP, Beck WD, Head E, Feldman DS, et al. 2010. Chromosome 21-derived microRNAs provide an etiological basis for aberrant protein expression in human Down syndrome brains. *J Biol Chem* **285**: 1529–1543.

Kujoth GC, Hiona A, Pugh TD, Someya S, Panzer K, Wohlgemuth SE, Hofer T, Seo AY, Sullivan R, Jobling WA, et al. 2005. Mitochondrial DNA mutations, oxidative stress, and apoptosis in mammalian aging. *Science* **309**: 481–484.

Kukat C, Wurm CA, Spåhr H, Falkenberg M, Larsson N-G, Jakobs S. 2011. Super-resolution microscopy reveals that mammalian mitochondrial nucleoids have a uniform size and frequently contain a single copy of mtDNA. *Proc Natl Acad Sci USA* **108**: 13534–13539.

Kuznetsov AV, Hermann M, Saks V, Hengster P, Margreiter R. 2009. The cell-type specificity of mitochondrial dynamics. *Int J Biochem Cell Biol* **41**: 1928–1939.

Kuznetsov AV, Margreiter R. 2009. Heterogeneity of mitochondria and mitochondrial function within cells as another level of mitochondrial complexity. *Int J Mol Sci* **10**: 1911–1929.

Lamberts SW, van den Beld AW, van der Lely AJ. 1997. The endocrinology of aging. *Science* **278**: 419–424.

Larsson N. 2010. Somatic mitochondrial DNA mutations in mammalian aging. *Annu Rev Biochem* **79**: 683–706.

Larsson N, Clayton D. 1995. Molecular genetic aspects of human mitochondrial disorders. *Annu Rev Genet* **29**: 151–178.

Larsson NG, Oldfors A. 2001. Mitochondrial myopathies. *Acta Physiol Scand* **171**: 385–393.

Larsson NG, Wang J, Wilhelmsson H, Oldfors A, Rustin P, Lewandoski M, Barsh GS, Clayton DA. 1998. Mitochondrial transcription factor A is necessary for mtDNA maintenance and embryogenesis in mice. *Nat Genet* **18**: 231–236.

Lee Y, Morrison BM, Li Y, Lengacher S, Farah MH, Hoffman PN, Liu Y, Tsingalia A, Jin L, Zhang P-W, et al. 2012. Oligodendroglia metabolically support axons and contribute to neurodegeneration. *Nature* **487**: 443–448.

Li SS. 1990. Human and mouse lactate dehydrogenase genes A (muscle), B (heart), and C (testis): protein structure, genomic organization, regulation of expression, and molecular evolution. *Prog Clin Biol Res* **344**: 75–99.

Loeb LA, Wallace DC, Martin GM. 2005. The mitochondrial theory of aging and its relationship to reactive oxygen species damage and somatic mtDNA mutations. *Proc Natl Acad Sci USA* **102**: 18769–18770.

Longley MJ, Nguyen D, Kunkel TA, Copeland WC. 2001. The fidelity of human DNA polymerase gamma with and without exonucleolytic proofreading and the p55 accessory subunit. *J Biol Chem* **276**: 38555–38562.

Longley MJ, Ropp PA, Lim SE, Copeland WC. 1998. Characterization of the native and recombinant catalytic subunit of human DNA polymerase gamma: identification of residues critical for exonuclease activity and dideoxynucleotide sensitivity. *Biochemistry* **37**: 10529–10539.

Lubec G, Engidawork E. 2002. The brain in Down syndrome (TRISOMY 21). *J Neurol* **249**: 1347–1356.

Luck DJ, Reich E. 1964. Dna in Mitochondria of Neurospora Crassa. *Proc Natl Acad Sci USA* **52**: 931–938.

Luft R, Ikkos D, Palmieri G, Ernster L, Afzelius B. 1962. A case of severe hypermetabolism of nonthyroid origin with a defect in the maintenance of mitochondrial respiratory control: a correlated clinical, biochemical, and morphological study. *J Clin Invest* **41**: 1776–1804.

Marazziti D, Baroni S, Picchetti M, Landi P, Silvestri S, Vatteroni E, Catena Dell'Osso M. 2011. Mitochondrial alterations and neuropsychiatric disorders. *Curr Med Chem* **18**: 4715–4721.

Margulis L. 1970. *Origin of eukaryotic cells*. Yale University Press, New Haven.

Markert CL, Shaklee JB, Whitt GS. 1975. Evolution of a gene. Multiple genes for LDH isozymes provide a model of the evolution of gene structure, function and regulation. *Science* **189**: 102–114.

Masoro EJ. 2005. Overview of caloric restriction and ageing. *Mech Ageing Dev* **126**: 913–922.

Mathews DH, Burkard ME, Freier SM, Wyatt JR, Turner DH. 1999. Predicting oligonucleotide affinity to nucleic acid targets. *RNA* **5**: 1458–1469.

McBride HM, Neuspiel M, Wasiak S. 2006. Mitochondria: more than just a powerhouse. *Curr Biol* **16**: R551–60.

McMillin JB, Dowhan W. 2002. Cardiolipin and apoptosis. *Biochim Biophys Acta* **1585**: 97–107.

Medawar PB. 1952. *An Unsolved Problem in Biology. Lewis, London. Reprinted in Medawar PB (1981) The Uniqueness of the Individual*.

Mereschkowski C. 1905. Über Natur und Ursprung der Chromatophoren im Pflanzenreiche. *Biol Centralbl* **25**: 593–604.

Michikawa Y, Mazzucchelli F, Bresolin N, Scarlato G, Attardi G. 1999. Aging-dependent large accumulation of point mutations in the human mtDNA control region for replication. *Science* **286**: 774–779.

Miura S. 1966. Lactic dehydrogenase isozymes of the brain. I. Electrophoretic studies on regional distribution and ontogenesis. *Folia Psychiatr Neurol Jpn* **20**: 337–347.

Murphy MP. 2009. How mitochondria produce reactive oxygen species. *Biochem J* **417**: 1–13.

Müller-Höcker J. 1990. Cytochrome c oxidase deficient fibres in the limb muscle and diaphragm of man without muscular disease: an age-related alteration. *J Neurol Sci* **100**: 14–21.

Müller-Höcker J. 1989. Cytochrome-c-oxidase deficient cardiomyocytes in the human heart--an age-related phenomenon. A histochemical ultracytochemical study. *Am J Pathol* **134**: 1167–1173.

Nass MM, Nass S. 1963. Intramitochondrial Fibers with Dna Characteristics. I. Fixation and Electron Staining Reactions. *J Cell Biol* **19**: 593–611.

Nicholls DG, Bernson VS, Heaton GM. 1978. The identification of the component in the inner membrane of brown adipose tissue mitochondria responsible for regulating energy dissipation. *Experientia Suppl* **32**: 89–93.

Nissen C, Schousboe A. 1979. Activity and isoenzyme pattern of lactate dehydrogenase in astroblasts cultured from brains of newborn mice. *J Neurochem* **32**: 1787–1792.

Niu X, Trifunovic A, Larsson N-G, Canlon B. 2007. Somatic mtDNA mutations cause progressive hearing loss in the mouse. *Exp Cell Res* **313**: 3924–3934.

Old SL, Johnson MA. 1989. Methods of microphotometric assay of succinate dehydrogenase and cytochrome c oxidase activities for use on human skeletal muscle. *Histochem J* **21**: 545–555.

Oliveira G, Diogo L, Grazina M, Garcia P, Ataíde A, Marques C, Miguel T, Borges L, Vicente AM, Oliveira CR. 2005. Mitochondrial dysfunction in autism spectrum disorders: a population-based study. *Dev Med Child Neurol* **47**: 185–189.

Öberg J, Spenger C, Wang F-H, Andersson A, Westman E, Skoglund P, Sunnemark D, Norinder U, Klason T, Wahlund L-O, et al. 2008. Age related changes in brain metabolites observed by 1H MRS in APP/PS1 mice. *Neurobiol Aging* **29**: 1423–1433.

Pagliarini DJ, Calvo SE, Chang B, Sheth SA, Vafai SB, Ong S-E, Walford GA, Sugiana C, Boneh A, Chen WK. 2008. A Mitochondrial Protein Compendium Elucidates Complex I Disease Biology. *Cell* **134**: 112–123.

Pettegrew JW, Keshavan MS, Minshew NJ. 1993. 31P nuclear magnetic resonance spectroscopy: neurodevelopment and schizophrenia. *Schizophr Bull* **19**: 35–53.

Piper MDW, Selman C, McElwee JJ, Partridge L. 2008. Separating cause from effect: how does insulin/IGF signalling control lifespan in worms, flies and mice? *J Intern Med* **263**: 179–191.

Provencher SW. 2001. Automatic quantitation of localized in vivo 1H spectra with LCModel. *NMR Biomed* **14**: 260–264.

Provencher SW. 1993. Estimation of metabolite concentrations from localized in vivo proton NMR spectra. *Magn Reson Med* **30**: 672–679.

Pryce JD, Gant PW, Saul KJ. 1970. Normal Concentrations of Lactate, Glucose, and Protein in Cerebrospinal Fluid, and the Diagnostic Implications of Abnormal Concentrations. *Clinical Chemistry* **16**: 562–565.

Rando TA, Chang HY. 2012. Aging, rejuvenation, and epigenetic reprogramming: resetting the aging clock. *Cell* **148**: 46–57.

Rodier F, Campisi J. 2011. Four faces of cellular senescence. *The Journal of Cell Biology* **192**: 547–556.

Romanick M. 2004. Long-lived Ames dwarf mouse exhibits increased antioxidant defense in skeletal muscle. *Mech Ageing Dev* **125**: 269–281.

Rose MR, Graves JL. 1989. What evolutionary biology can do for gerontology. *J Gerontol* **44**: B27–9.

Ross JM, Coppotelli G, Olson L. 2011. Reply to Quistorff and Grunnet: Dysfunctional mitochondria, brain lactate, and lactate dehydrogenase isoforms. *Proc Natl Acad Sci USA* **108**: E22–E22.

Rowe J, Kahn R. 1987. Human aging: usual and successful. *Science* **237**: 143–149.

Ruiz-Pesini E, Lott MT, Procaccio V, Poole JC, Brandon MC, Mishmar D, Yi C, Kreuziger J, Baldi P, Wallace DC. 2007. An enhanced MITOMAP with a global mtDNA mutational phylogeny. *Nucleic Acids Res* **35**: D823–8.

Sadler ME, Miller CJ, Christensen K, McGue M. 2011. Subjective wellbeing and longevity: a co-twin control study. *Twin Res Hum Genet* **14**: 249–256.

Safdar A, Bourgeois JM, Ogborn DI, Little JP, Hettinga BP, Akhtar M, Thompson JE, Melov S, Mocellin NJ, Kujoth GC, et al. 2011. Endurance exercise rescues progeroid aging and induces systemic mitochondrial rejuvenation in mtDNA mutator mice. *Proc Natl Acad Sci USA* **108**: 4135–4140.

Samorajski T, Friede RL, Ordy JM. 1971. Age differences in the ultrastructure of axons in the pyramidal tract of the mouse. *J Gerontol* **26**: 542–551.

Sardi F, Fassina L, Venturini L, Inguscio M, Guerriero F, Rolfo E, Ricevuti G. 2011. Alzheimer's disease, autoimmunity and inflammation. The good, the bad and the ugly. *Autoimmun Rev* **11**: 149–153.

Schatz G, Haslbrunner E, Tuppy H. 1964. Deoxyribonucleic acid associated with yeast mitochondria. *Biochem Biophys Res Commun* **15**: 127–132.

Schon EA, Kim SH, Ferreira JC, Magalhães P, Grace M, Warburton D, Gross SJ. 2000. Chromosomal non-disjunction in human oocytes: is there a mitochondrial connection? *Hum Reprod* **15 Suppl 2**: 160–172.

Schwarze SR, Lee CM, Chung SS, Roecker EB, Weindruch R, Aiken JM. 1995. High levels of mitochondrial DNA deletions in skeletal muscle of old rhesus monkeys. *Mech Ageing Dev* **83**: 91–101.

Seligman AM. 1968. Nondroplet Ultrastructural Demonstration of Cytochrome Oxidase Activity with a Polymerizing Osmiophilic Reagent, Diaminobenzidine (Dab). *The Journal of Cell Biology* **38**: 1–14.

Shlomai J. 2010. Redox control of protein-DNA interactions: from molecular mechanisms to significance in signal transduction, gene expression, and DNA replication. *Antioxid Redox Signal* **13**: 1429–1476.

Sickevitz P. 1957. Powerhouse of the cell. *Scientific American*.

Smeitink J, van den Heuvel L, DiMauro S. 2001. The genetics and pathology of oxidative phosphorylation. *Nat Rev Genet* **2**: 342–352.

Soong NW, Hinton DR, Cortopassi G, Arnheim N. 1992. Mosaicism for a specific somatic mitochondrial DNA mutation in adult human brain. *Nat Genet* **2**: 318–323.

Stacpoole PW. 2012. The pyruvate dehydrogenase complex as a therapeutic target for age-related diseases. *Aging Cell* **11**: 371–377.

Stewart JB, Freyer C, Elson JL, Wredenberg A, Cansu Z, Trifunovic A, Larsson N-G. 2008. Strong purifying selection in transmission of mammalian mitochondrial DNA. *PLoS Biol* **6**: e10.

Strick TR, Croquette V, Bensimon D. 2000. Single-molecule analysis of DNA uncoiling by a type II topoisomerase. *Nature* **404**: 901–904.

Stumpf JD, Copeland WC. 2011. Mitochondrial DNA replication and disease: insights from DNA polymerase γ mutations. *Cell Mol Life Sci* **68**: 219–233.

Taber R, Irwin S. 1969. Anesthesia in Mouse. *Fed Proc* **28**: 1528–1532.

Tanhauser S, Laipis P. 1995. Multiple Deletions Are Detectable in Mitochondrial-Dna of Aging Mice. *J Biol Chem* **270**: 24769–24775.

Taylor RW, Barron MJ, Borthwick GM, Gospel A, Chinnery PF, Samuels DC, Taylor GA, Plusa SM, Needham SJ, Greaves LC, et al. 2003a. Mitochondrial DNA mutations in human colonic crypt stem cells. *J Clin Invest* **112**: 1351–1360.

Taylor RW, McDonnell MT, Blakely EL, Chinnery PF, Taylor GA, Howell N, Zeviani M, Briem E, Carrara F, Turnbull DM. 2003b. Genotypes from patients indicate no paternal mitochondrial DNA contribution. *Ann Neurol* **54**: 521–524.

Tkáč I, Starcuk Z, Choi IY, Gruetter R. 1999. In vivo 1H NMR spectroscopy of rat brain at 1 ms echo time. *Magn Reson Med* **41**: 649–656.

Trifunovic A, Hansson A, Wredenberg A, Rovio AT, Dufour E, Khvorostov I, Spelbrink JN, Wibom R, Jacobs HT, Larsson N-G. 2005. Somatic mtDNA mutations cause aging phenotypes without affecting reactive oxygen species production. *Proc Natl Acad Sci USA* **102**: 17993–17998.

Trifunovic A, Wredenberg A, Falkenberg M, Spelbrink JN, Rovio AT, Bruder CE, Bohlooly-Y M, Gidlöf S, Oldfors A, Wibom R, et al. 2004. Premature ageing in mice expressing defective mitochondrial DNA polymerase. *Nature* **429**: 417–423.

Tulinius MH, Holme E, Kristiansson B, Larsson NG, Oldfors A. 1991. Mitochondrial encephalomyopathies in childhood. I. Biochemical and morphologic investigations. *J Pediatr* **119**: 242–250.

Verge B, Alonso Y, Valero J, Miralles C, Vilella E, Martorell L. 2011. Mitochondrial DNA (mtDNA) and schizophrenia. *Eur Psychiatry* **26**: 45–56.

Vermulst M, Wanagat J, Kujoth GC, Bielas JH, Rabinovitch PS, Prolla TA, Loeb LA. 2008. DNA deletions and clonal mutations drive premature aging in mitochondrial mutator mice. *Nat Genet* **40**: 392–394.

Voet D, Voet JG, Pratt CW. 2012. *Fundamentals of Biochemistry*. Wiley.

Vrinten DH, Hamers FFT. 2003. “CatWalk” automated quantitative gait analysis as a novel method to assess mechanical allodynia in the rat; a comparison with von Frey testing. *Pain* **102**: 203–209.

Wallace DC. 2005. A mitochondrial paradigm of metabolic and degenerative diseases, aging, and cancer: a dawn for evolutionary medicine. *Annu Rev Genet* **39**: 359–407.

Wallace DC. 1999. Mitochondrial Diseases in Man and Mouse. *Science* **283**: 1482–1488.

Wallace DC. 2007. Why do we still have a maternally inherited mitochondrial DNA? Insights from evolutionary medicine. *Annu Rev Biochem* **76**: 781–821.

Wang Y, Bontempi B, Hong SM, Mehta K, Weinstein PR, Abrams GM, Liu J. 2008. A comprehensive analysis of gait impairment after experimental stroke and the therapeutic effect of environmental enrichment in rats. *J Cereb Blood Flow Metab* **28**: 1936–1950.

Weindruch R. 1996. The retardation of aging by caloric restriction: studies in rodents and primates. *Toxicol Pathol* **24**: 742–745.

Weismann A. 1889. *Essays upon Heredity and Kindred Biological Problems.* Oxford University Press.

Weissman JR, Kelley RI, Bauman ML, Cohen BH, Murray KF, Mitchell RL, Kern RL, Natowicz MR. 2008. Mitochondrial disease in autism spectrum disorder patients: a cohort analysis. *PLoS ONE* **3**: e3815.

Williams GC. 1957. Pleiotropy, natural selection, and the evolution of senescence. *Evolution* **11**: 398–411.

Willis BL, Gao A, Leonard D, Defina LF, Berry JD. 2012. Midlife Fitness and the Development of Chronic Conditions in Later Life. *Arch Intern Med* 1–8.

Wilson PD, Franks LM. 1975. The effect of age on mitochondrial ultrastructure and enzyme cytochemistry. *Biochem Soc Trans* **3**: 126–128.

Winnefeld M, Lyko F. 2012. The aging epigenome: DNA methylation from the cradle to the grave. *Genome Biol* **13**: 165.

Wolf J, Weinberger B, Arnold CR, Maier AB, Westendorp RGJ, Grubeck-Loebenstein B. 2012. The effect of chronological age on the inflammatory response of human fibroblasts. *Exp Gerontol* **47**: 749–753.

Yao J, Hamilton RT, Cadenas E, Brinton RD. 2010. Decline in mitochondrial bioenergetics and shift to ketogenic profile in brain during reproductive senescence. *Biochim Biophys Acta* **1800**: 1121–1126.

Yasuda K, Ishii T, Suda H, Akatsuka A, Hartman PS, Goto S, Miyazawa M, Ishii N. 2006. Age-related changes of mitochondrial structure and function in Caenorhabditis elegans. *Mech Ageing Dev* **127**: 763–770.

Yasuhara T, Hara K, Maki M, Masuda T, Sanberg CD, Sanberg PR, Bickford PC, Borlongan CV. 2008. Dietary supplementation exerts neuroprotective effects in ischemic stroke model. *Rejuvenation Res* **11**: 201–214.

Yesavage JA, Holman CA, Berger PA. 1982a. Cerebrospinal fluid lactate levels and aging: findings in normals and patients with major depressive disorders. *Gerontology* **28**: 377–380.

Yesavage JA, Holman CA, Sarnquist FH, Berger PA. 1982b. Elevation of cerebrospinal fluid lactate with aging in subjects with normal blood oxygen saturations. *J Gerontol* **37**: 313–315.

Yu GL, Bradley JD, Attardi LD, Blackburn EH. 1990. In vivo alteration of telomere sequences and senescence caused by mutated Tetrahymena telomerase RNAs. *Nature* **344**: 126–132.

Zhang DX, Gutterman DD. 2007. Mitochondrial reactive oxygen species-mediated signaling in endothelial cells. *Am J Physiol Heart Circ Physiol* **292**: H2023–31.

Zhang X, Liu H, Wu J, Zhang X, Liu M, Wang Y. 2009. Metabonomic alterations in hippocampus, temporal and prefrontal cortex with age in rats. *Neurochem Int* **54**: 481–487.

Zick M, Rabl R, Reichert AS. 2009. Cristae formation-linking ultrastructure and function of mitochondria. *Biochim Biophys Acta* **1793**: 5–19.

Zuker M. 2003. Mfold web server for nucleic acid folding and hybridization prediction. *Nucleic Acids Res* **31**: 3406–3415.